Design and Testing of Three-Axis Satellite Attitude Determination and Stabilization Systems that are Based on Magnetic Sensing and Actuation

Final Technical Report for AFOSR GRANT F49620-01-1-0117

by Mark L. Psiaki

Sibley School of Mechanical and Aerospace Engineering

Cornell University, Ithaca, N.Y. 14853-7501

and Moshe Guelman

Faculty of Aerospace Engineering

The Technion, Haifa, 32000 Israel

Abstract

Three-axis satellite attitude determination and active stabilization systems have been designed and tested using both flight experiments and simulation studies. These are being developed for use on low-Earth-orbiting nano-satellites. Such satellites can be used as elements of constellations that implement synthetic aperture radar or that serve as nodes in a communications network. The research has addressed the problems of under-sensing and under-actuation that are present in magnetic-based systems. Magnetometer outputs are insensitive to rotation about the local Earth magnetic field, and magnetic torque coils cannot produce torque along the field direction. A new attitude representation and a special globally-convergent extended Kalman filter have been used to solve the 3-axis attitude estimation problem. The efficacy of this system has been demonstrated using data from two missions, the Hubble Space Telescope and the Far-Ultraviolet Spectroscopic Explorer. Semi-active global 3-axis stabilization has been demonstrated using a simplified magnetometer output feedback control law

REPORT DOCUMENTATION PAGE

Form Approved
OMB No. 0704-0188

1. REPORT DATE *(DD-MM-YYYY)*	**2. REPORT TYPE**	**3. DATES COVERED** *(From - To)*
27-11-2002	final	1-01-2001 to 31-08-2002

4. TITLE AND SUBTITLE
Design and Testing of Three-Axis Satellite Attitude Determination and Stabilization Systems that are Based on Magnetic Sensing and Actuation

5a. CONTRACT NUMBER

5b. GRANT NUMBER
F49620-01-1-0117

5c. PROGRAM ELEMENT NUMBER

6. AUTHOR(S)
Psiaki, Mark L.; Guelman, Moshe

5d. PROJECT NUMBER

5e. TASK NUMBER

5f. WORK UNIT NUMBER

7. PERFORMING ORGANIZATION NAME(S) AND ADDRESS(ES)

Cornell University
Office of Sponsored Programs
115 Day Hall
Ithaca, NY 14853-2801

Research Authority
Technion R&D Foundation
Technion City, Haifa
32000 Israel

8. PERFORMING ORGANIZATION REPORT NUMBER
Technion Report No. 2002.07

9. SPONSORING / MONITORING AGENCY NAME(S) AND ADDRESS(ES)
AFOSR/NM
801 N. Randolph St., Rm. 732
Arlington, VA 22203

10. SPONSOR/MONITOR'S ACRONYM(S)

11. SPONSOR/MONITOR'S REPORT NUMBER(S)

12. DISTRIBUTION / AVAILABILITY STATEMENT
A – Approved for public release; distribution unlimited.

13. SUPPLEMENTARY NOTES

14. ABSTRACT
Three-axis satellite attitude determination and active stabilization systems have been designed and tested using both flight experiments and simulation studies. These are being developed for use on low-Earth-orbiting nano-satellites. Such satellites can be used as elements of constellations that implement synthetic aperture radar or that serve as nodes in a communications network. The research has addressed the problems of under-sensing and under-actuation that are present in magnetic-based systems. Magnetometer outputs are insensitive to rotation about the local Earth magnetic field, and magnetic torque coils cannot produce torque along the field direction. A new attitude representation and a special globally-convergent extended Kalman filter have been used to solve the 3-axis attitude estimation problem. The efficacy of this system has been demonstrated using data from two missions, the Hubble Space Telescope and the Far-Ultraviolet Spectroscopic Explorer. Semi-active global 3-axis stabilization has been demonstrated using a simplified magnetometer output feedback control law in combination with weak passive stabilization of two axes. The passive stabilization can come from a very small momentum wheel or from a new aerodynamic system. The momentum-wheel-based concept has been successfully tested on the TechSat Gurwin II spacecraft.

15. SUBJECT TERMS
Satellite Attitude Determination; Satellite Attitude Control; Magnetic Torque Rods; Magnetometers; Magnetic Attitude Control

16. SECURITY CLASSIFICATION OF:			**17. LIMITATION OF ABSTRACT**	**18. NUMBER OF PAGES**	**19a. NAME OF RESPONSIBLE PERSON**
a. REPORT	**b. ABSTRACT**	**c. THIS PAGE**		53	**19b. TELEPHONE NUMBER** *(include area code)*

in combination with weak passive stabilization of two axes. The passive stabilization can come from a very small momentum wheel or from a new aerodynamic system. The momentum-wheel-based concept has been successfully tested on the TechSat Gurwin II spacecraft.

1.0 Introduction

1.1 Goals of Research

This research had two goals. One was to develop and test attitude determination and stabilization systems that are appropriate for use on small satellites that constitute parts of constellations. The other was to develop high-fidelity MATLAB simulations of open-loop and closed-loop satellite attitude dynamics.

The new attitude estimation and stabilization systems use the Earth's magnetic field for sensing and actuation. Magnetometer sensing and magnetic torque coil actuation are attractive for use on small satellites in Low Earth Orbit (LEO) because of these devices' light weight, low power consumption, and high reliability. They are difficult to use, however, because they are two-axis devices. Geometry and physics dictate that magnetic systems provide sensing and actuation only about the two axes that are perpendicular to the local magnetic field. The estimation and feedback stabilization problems, on the other hand, are concerned with all three attitude angles, i.e., roll, pitch, and yaw, and with all three attitude rates. Fortunately, the magnetic field moves with respect to inertial space in most LEO applications. This motion makes the 3rd axis observable and controllable in a theoretical sense. Practically, however, robustness issues can militate against the exploitation of observability and controllability because typical estimators and controllers that exploit these properties rely on dynamic models of uncertain validity. The main goal of this part of the research has been to overcome these limitations and create full 3-axis

estimation and stabilization systems based only on magnetics. A second goal has been to prove the techniques by testing them on actual spacecraft.

The MATLAB attitude simulation software has been designed to provide a highly flexible high-fidelity means of testing new concepts for attitude determination and control systems. The use of open-source MATLAB .m-files creates flexibility. The incorporation of a variety of disturbance torque models causes the simulation to be high-fidelity. These models include torques due to gravity-gradient effects, residual magnetic dipole moments, solar radiation pressure, Earth albedo radiation pressure, and aerodynamic drag and lift. These torque models take into account the details of the spacecraft's geometry and inertial properties, and they include the physics of how the Earth's gravitational field, the upper atmosphere, solar radiation, and the Earth's albedo act on the spacecraft's components.

1.2 Relationship of Research to Needs of Air Force and Department of Defense Programs

The results of this research are relevant to the Air Force's mission because they advance the state of the art of attitude estimation, stabilization, and control for small spacecraft. These systems are practical for use on small spacecraft because they reduce the number, weight, and power of the sensors, actuators, and passive stabilization devices that are needed. Such systems would be ideal for a constellation of small, simple, light-weight LEO spacecraft.

Attitude determination and pointing accuracies on the order of several degrees have been demonstrated via flight-experiments, post-flight data processing, and simulation. These accuracies are achievable in the presence of significant disturbance torques and system modeling errors. These levels of accuracy will enable the design of very small, light-weight spacecraft that have performance capabilities which can be exploited to perform missions such as remote sensing or establishment of a communications network.

1.3 Summary of this Project's Efforts and Accomplishments

Four efforts have been pursued during the grant period. The first attempted to test a local magnetic-torquer-based attitude controller on the TechSat Gurwin II spacecraft [1]. The performance of an existing controller at near-zero momentum bias has been demonstrated, but the new local controller could not be tested because of actuator-sensor cross-talk problems when the momentum wheel was stopped. The near-zero momentum bias test was significant because it showed that momentum bias designs can be implemented using momentum wheels that store 70 to 200 times less angular momentum than is typically used in current practice for a spacecraft of similar dimensions.

The second effort developed a globally convergent attitude and rate estimator that uses only magnetometer data. This new estimator has been tested successfully using simulation data and using actual flight data from NASA's Hubble Space Telescope (HST) and Far-Ultraviolet Spectroscopic Explorer (FUSE) missions.

The third effort sought to develop globally convergent magnetic-torquer-based attitude controllers. One approach was based on a projection of Mortensen's globally stable control law [2] onto the subspace perpendicular to the magnetic field. Simulations showed that this controller works for the nearly symmetric TechSat Gurwin II spacecraft, but a global convergence proof could not be derived. An alternate approach attempted to expand on Holden and Lawrence's [3] Lyapunov-based nutation damper. This attempt failed because there are significant disturbance torques that cause Lyapunov stability to break down when the spacecraft attempts to point towards nadir. Preliminary work was done on a sliding-mode-type global controller, but this work could not be completed before the grant ended.

The fourth effort has been the development of a MATLAB spacecraft attitude dynamics simulation package. This package has been used in conjunction with the other three efforts as an evaluation tool.

1.4 Outline of Report

The remainder of this report consists of 3 sections. Section 2 gives a break down of the personnel involved on the project and describes the publications that are being prepared based on this work. Section 3 presents significant results from the different studies that have been carried out as part of this project. Section 4 is a summary of this report.

2.0 Personnel and Publications

Five different researchers have been involved in this project. Prof. Mark Psiaki, the principal investigator, is a faculty member in Cornell's Sibley School of Mechanical and Aerospace Engineering. The other four investigators are all associated with the Asher Space Research Institute at the Technion in Haifa, Israel. They are Prof. Moshe Guelman, Dr. Alexander Shiryaev and Roni Waller, both of whom are research engineers, and Mark Rozanov, who was an undergraduate in the Technion's Faculty of Aerospace Engineering during the grant period. Prof. Psiaki worked on development of the linearized control laws for testing on the Technion's TechSat Gurwin II spacecraft, he developed the new 3-axis attitude determination algorithm and the MATLAB attitude dynamics simulation, he tested the attitude determination algorithm, and he carried out the attempts to develop a globally stabilizing magnetic controller. Prof. Guelman and Dr. Shiryaev helped to design the various controllers that were flight tested on the TechSat Gurwin II spacecraft, they oversaw the tests, and they evaluated the results. Mr. Waller wrote the flight software for the flight tests, conducted the actual tests, and collected telemetry data from the tests.

Mr. Rozanov assisted in simulation-based evaluation of flight controllers as they were being developed.

Two archival publications are planned based on this work. The first describes the magnetometer-based 3-axis attitude determination system and presents test results using actual flight data [4]. It is currently in preparation. The second paper will report on a new aerodynamic/magnetic active 3-axis attitude stabilization system for use below 500 km altitude. Some of the work on this latter topic was performed under different support, but this planned publication is being cited here for two reasons. First, this new system uses a magnetometer-to-magnetic-torquer feedback control law that is very similar to the one which has been used on the TechSat Gurwin II spacecraft during the flight experiments. The success of these flight experiments was the primary reason why this control law was incorporated into the new system. Second, the new system's drag-based passive pitch-yaw stabilization system was designed based primarily on the aerodynamic torque simulation that was developed under this grant.

3.0 Research Results

3.1 Experimental Demonstration of Low-Momentum-Bias Magnetic Attitude Control

Although the experimental flight-test program did not produce all of the desired results, it demonstrated a significant advance in the state of the art of attitude control: the ability to do 3-axis stabilization of a momentum-bias spacecraft with a very low momentum bias. A momentum bias spacecraft is a nadir-pointing spacecraft that includes a pitch-axis angular momentum wheel in order to establish gyroscopic roll-yaw stability. Typical designs use a momentum wheel whose angular momentum is 70 to 200 times as large as the angular momentum that results from the pitch inertia and the nominal once-per-orbit pitch-axis rotation rate [5,6]. As part of the present work, the TechSat Gurwin II spacecraft has been controlled successfully with a momentum bias that is only

0.9 times the nominal pitch angular momentum. This value is more than 75 times smaller than the next smallest momentum bias that is reported in the literature.

This performance has been achieved by using the TechSat's compass magnetic attitude controller. It is a time-varying output feedback controller. It compares the spacecraft-axes measured magnetic field vector time history to the reference time history that would result if the attitude were correct. The error vector gets fed back to the magnetic torque rods using a simple PD control law. It is called the compass algorithm because the proportional control terms effectively implement a compass-needle-type stabilization. The magnetic torque directly stabilizes the two axes that are perpendicular to the magnetic field via a high-bandwidth feedback loop. The axis that is parallel to the field gets stabilized by the momentum wheel because the field rotates with respect to inertial coordinates as the spacecraft progresses along its orbit. Any non-zero error along the field eventually forces the momentum wheel to precess about an axis that is perpendicular to its spin axis, but the wheel resists precession in a way that tends to null out attitude errors which are parallel to the field.

The relevance of this work to Air Force and civilian missions is that it allows the use of smaller momentum wheels. This will make momentum-bias designs more practical on micro- and nano-satellites because they will not need to devote a significant fraction of their bus weight and power to the momentum wheel due to its greatly reduced size.

The results of this study are more thoroughly reported in Appendix A of this report. This appendix contains the final sub-contractor report that has been submitted to Cornell University by the Technion.

3.2 Globally-Convergent 3-Axis Attitude and Rate Estimation Based only on Magnetometer Data

A globally convergent attitude determination filter has been developed to estimate 3-axis attitude and attitude rate from magnetometer data only. The attitude determination algorithm uses implicit Euler dynamics to propagate attitude rate estimates. It expands on the iterated extended Kalman filter (EKF) concept in order to deal with the important nonlinearities. In addition, it uses a global initialization strategy that starts with a number of filters which cover the 2-dimensional box of significant initial condition uncertainty. Hypothesis testing is used to eliminate all but one of the filters after the best one has reached steady state.

The new filter works with a special attitude representation. This representation starts with the minimum-rotation quaternion that aligns the inertial magnetic field with the measured magnetic field in spacecraft coordinates. The attitude is parameterized by 3 quantities that define a rotation from this quaternion to the true spacecraft attitude. One attitude parameter is a rotation about the magnetic field, which can be large. The other two parameters are rotations perpendicular to the magnetic field, which are guaranteed to be small. The smallness of these latter two angles guarantees that the representation avoids its singularity.

The principal uncertainties in attitude and attitude rate are in the direction of rotation about the instantaneous magnetic field vector, and the unique parts of this filter have been developed to address this issue. The iterated EKF linearizes with respect to the small unknown rotations that are perpendicular to the magnetic field, but it performs a global numerical least-squares optimization with respect to the unknown rotation about the magnetic field. This numerical optimization involves the nonlinearities of both the measurement model and the dynamics model. The global initialization strategy starts multiple filters at grid points that span a square in the two-

dimensional space of the unknown rotations about the magnetic field at the first two measurement samples. If the grid is chosen fine enough, then one of the filters will start with an initial condition that is close to the true attitude and rate. This filter will produce the smallest cumulative cost in its square-root information filter least-squares cost function, and this cost can be used to identify that filter's initial grid point as the most reasonable hypothesis about the initial conditions.

This filter has been tested off-line using data form the HST and FUSE missions. Steady-state attitude and rate accuracies on the order of 4 deg and 50 arcsec/sec 3-s have been achieved on FUSE, Fig. 1. There are hopes to achieve even better accuracies with improved magnetic torque rod data. HST accuracies are believed to be on the order of 8 deg and 20 arcsec/sec 3-s. It is not possible to ascertain the true HST accuracy because there is no "truth" standard from an accurate measurement system for the HST data sets, which were taken from a time in late 1999 when HST was operating in its zero-gyro sun-pointing mode due to rate-gyro failures.

This filter could be important to almost any Air Force or civilian mission. Almost all spacecraft carry a magnetometer. This filter provides a robust full 3-axis back-up mode attitude and rate determination capability that will be useful in the likely event that other sensors may fail, sensors such as rate gyros, horizon scanners, sun sensors, or star trackers. More importantly, this system could be chosen to serve as the primary attitude determination system for a low-weight, low-budget, low-accuracy mission such as a single element of a large constellation of spacecraft.

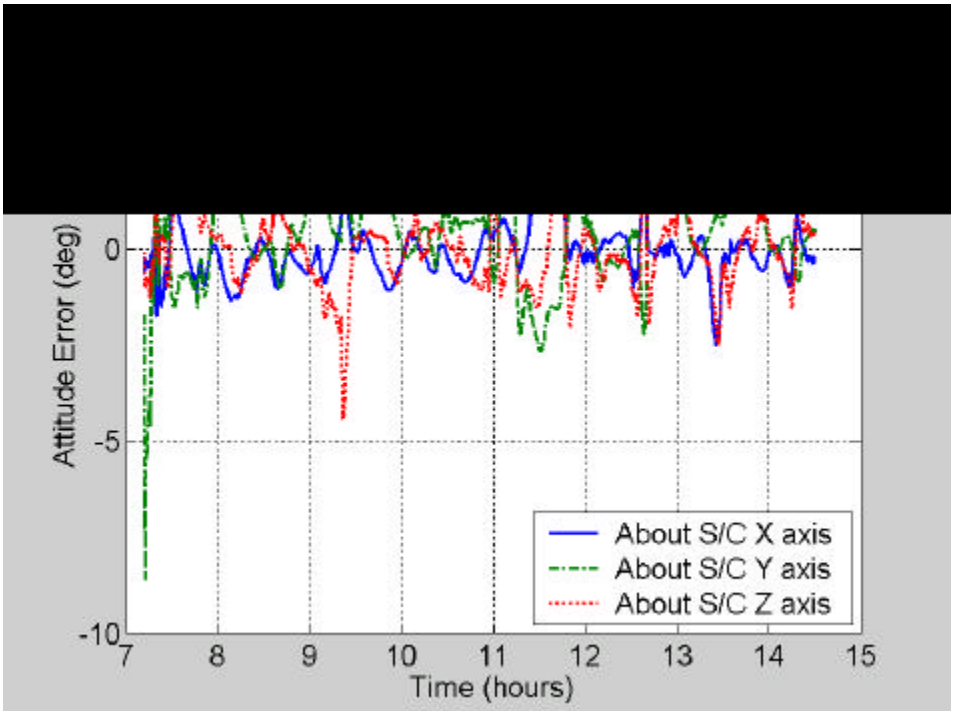

Fig. 1. Attitude error time histories for the globally convergent magnetometer-based attitude estimator when operating on FUSE data.

3.3 Aerodynamic/Active-Magnetic Stabilization of a Nano-Satellite

Work on the drag torque model, when coupled with a project at Cornell do design a 1 kg nano-satellite, has lead to a new 3-axis attitude stabilization design. The genesis of the design came from the fact that aerodynamic drag torque tends to overwhelm all other environmental torques at altitudes of 400 km and below. This was the target altitude range for the Cornell nano-satellite. The original design planned to use gravity-gradient stabilization for the roll and pitch axes, but it proved difficult to design a light-weight system that did not get overwhelmed by the aerodynamic drag torque about the pitch axis.

The new design turns the drag torque into an asset rather than a liability. It stabilizes yaw and pitch by using a badminton-birdie type configuration, one like that pictured in Fig. 2. The basic principal of operation is the same as that of a birdie: A pitch or yaw rotation will vary the

frontal area of each "feather," which changes its net drag force. Pitch and yaw rotations also modulate the effective moment arm of each "feather's" drag force as measured with respect to the center of mass. These variations cause restoring torques about the pitch and yaw axes. The "birdie's" deployable "feathers" can be made out of thin, light-weight strips of metal or Kevlar that resemble the tape in a carpenter's retractable tape measure.

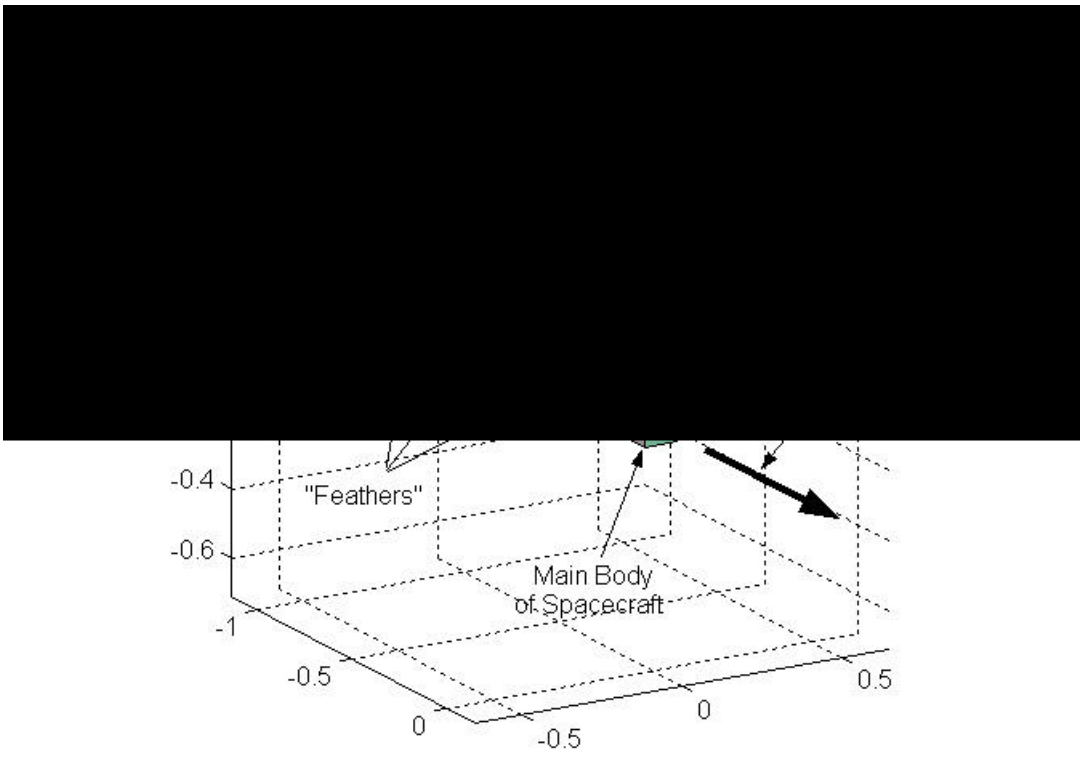

Fig. 2. Badminton-birdie-type spacecraft pitch-yaw stabilization system configuration.

The actual torque produced has been calculated using a panel model of the main spacecraft and the feathers. An aerodynamic model valid at high-Knudsen number has been used [7]. It computes the pressure and tangential stress on each surface as functions of the dynamic pressure, the air-relative velocity direction in spacecraft-referenced coordinates, the dimensionless airspeed

and down-wash as non-dimensionalized by the upper atmosphere's thermal energy, and the spacecraft's surface temperature.

An active magnetic damping and roll stabilization system has been developed for the birdie-type spacecraft in order to achieve full 3-axis nadir-pointing stabilization. The aerodynamic torque provides no roll stiffness and almost no damping. The active magnetic controller makes up for these deficiencies. It is an output feedback system that is very much like the TechSat Gurwin II's *COMPASS* control law, which is defined in eq. (14) of Appendix A. The birdie's controller compares the measured magnetic field in spacecraft coordinates with the magnetic field in local-level coordinates. It feeds back any error through a proportional-integral-derivative control law that drives the magnetic torque rods' dipole moment vector. The goal of this controller is to align the spacecraft coordinate system with the local-level coordinate system so that the spacecraft will point towards nadir. This controller has been shown to produce global three-axis stability if two axes are passively stabilized. The roll and yaw axes are passively stabilized by the momentum wheel in the case of TechSat Gurwin II's nominal attitude stabilization system. In the case of the birdie system, the aerodynamic torque provides the necessary passive stabilization to the pitch and yaw axes.

A simulation study has demonstrated that this system provides global 3-axis stabilization and that it can counteract the expected disturbance torques. The principal disturbance torques are gravity-gradient torques, pitch and yaw drag torques due to center-of-mass imbalance, and roll torques due to shape asymmetry (twist of the feathers) and slight aerodynamic lift effects. Global stabilization can be achieved for altitudes up to 500 km. A typical plot of the transient decay from tumbling motion to 3-axis stabilized motion is shown in Fig. 3.

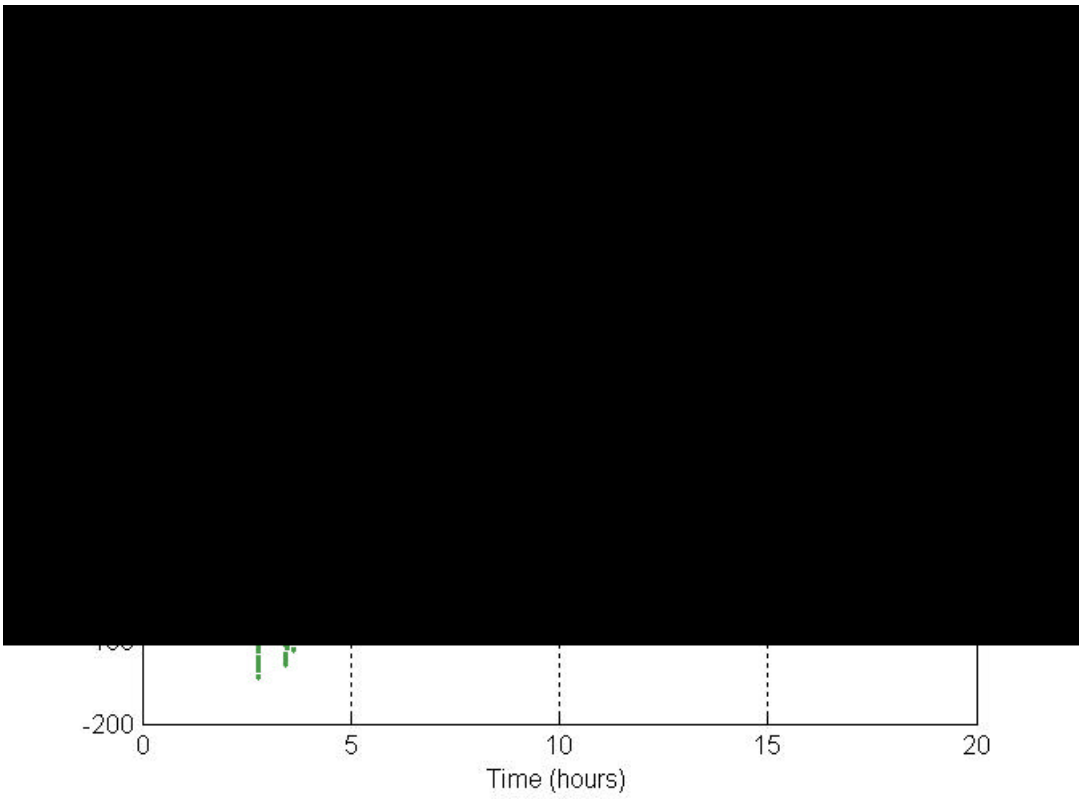

Fig. 3. Closed-loop "birdie" transient attitude response starting from an initial tumble of 3°/sec in roll, -4°/sec in pitch, and 2°/sec in yaw.

4.0 Summary

New satellite attitude determination and active stabilization methods have been developed for use on constellations of small satellites. These methods make use of magnetic sensing and actuation in order to reduce the weight and power of the required components. The resulting under-sensed/under-actuated estimation and control problems have been addressed using concepts from modern control theory.

A successful 3-axis attitude determination system has been developed by working with a new attitude representation that has been specially tailored to separate the easy and hard parts of the estimation problem. The system is a custom-designed iterated extended Kalman filter. It incorporates a hypothesis-testing strategy that enables it to achieve global convergence, which is

necessary for autonomous operation. This system has been successfully tested using flight data from NASA's HST and FUSE missions. Its 3-s accuracy is on the order of 4 deg per axis, and better accuracy may be achievable with improved dynamic models and improved magnetometers.

Active magnetic control laws have been developed to globally stabilize all 3 axes of a nadir-pointing spacecraft despite the under-actuated nature of the problem. Successful designs have been tested, both in-flight aboard the TechSat Gurwin II spacecraft and via simulation. In addition to active magnetic stabilization, these designs require weak passive stabilization of two axes. One design uses a very low momentum pitch wheel for passive roll-yaw stabilization. A second design uses a new passive aerodynamic pitch-yaw stabilization system. This latter system is based on the concept of a badminton birdie and can be used at altitudes below 500 km. Only the former system has been tested in actual flight.

A high fidelity attitude dynamics simulation has also been developed. This simulation includes a panel model of the aerodynamic and solar-radiation pressure torques. It has been used to test all of the system concepts that have been considered under this grant.

References

1. Psiaki, M.L., "Magnetic Torquer Attitude Control via Asymptotic Periodic Linear Quadratic Regulation," *Journal of Guidance, Control, and Dynamics*, Vol. 24, No. 2, 2001, pp. 386-394.

2. Mortensen, R.E., "A Globally Stable Linear Attitude Regulator," *International Journal of Control*, Vol. 8, No. 3, 1968, pp. 297-302.

3. Holden, T.E., and Lawrence, D.A., "A Lyapunov Design Approach to Magnetic Nutation Damping," *Proceedings of the AIAA Guidance, Navigation, and Control Conf.*, Portland, OR, 9-11 August 1999, pp. 146-154.

4. Psiaki, M.L., "A Global Method for Magnetometer-Based 3-Axis Spacecraft Attitude Determination," in preparation for submission to the *Journal of Guidance, Control, and Dynamics*.

5. Alfriend, K.T., "Magnetic Attitude Control System for Dual-Spin Satellites," *AIAA Journal*, Vol. 13, No. 6, 1975, pp. 817-822.

6. Hablani, H.B., "Comparative Stability Analysis and Performance of Magnetic Controllers for Bias Momentum Satellites," *Journal of Guidance, Control, and Dynamics*, Vol. 18, No. 6, 1995, pp. 1313-1320.

7. Gombosi, T.I., *Gaskinetic theory*, Cambridge University Press, (New York, 1994), pp. 227-261.

TECHNION - ISRAEL INSTITUTE OF TECHNOLOGY

Norman and Helen Asher
Space Research Institute

Design And Experimental Testing Of Three-Axis Satellite Attitude Control Systems That Use Only Magnetic Torquers

FINAL REPORT Sub-Contract No. 37687-6503

by

A. Shiryaev, R. Waller, M. Rozanov, M. Guelman

Report No. 2002.07 **June 2002**

Design And Experimental Testing Of Three-Axis Satellite Attitude Control Systems That Use Only Magnetic Torquers

by

A. Shiryaev, R. Waller, M. Rozanov, M. Guelman

Abstract

A study was performed on control algorithms intended to provide three-axis stabilization of a satellite, equipped with a magnetometer as the only sensor, and three-axis magneto-torquers as the only actuators. Two different attitude control algorithms were considered, namely *Linear Quadratic Regulator* and *No Wheel controller*. The ability of these algorithms to achieve the required performance was tested by multiple numerical simulations, under various initial conditions and different scenarios. The implementation of the new controllers onboard the TechSat satellite proved to be a complicated task, mainly because of insufficient pre-flight testing of the onboard equipment, which resulted in the inability to build up an adequate model of the perturbing torques affecting the satellite's attitude dynamics. Still, important results were obtained both on control laws able to provide three-axis stabilization of the satellite even with a *very small* momentum bias as well as the ability to implement *very efficient* Kalman filters, to fully estimate the satellite's attitude, as confirmed by TechSat actual flight tests.

Acronyms

BF – Body Frame

GE – Ground Estimator

GMF – Geomagnetic Field

IF – Inertial Frame

EKF – Extended Kalman Filter

LKF – Linear Kalman Filter

LQR– Linear Quadratic Regulator

MGM – Magnetometer

MW – Momentum Wheel

PMC – Purely Magnetic Control

TF – Trajectory Frame

1. Introduction

The scope of the report is implementation and flight tests of a purely magnetic satellite's attitude control (PMC) algorithms that use a magnetometer (MGM) as the only sensor, and 3-axis magneto-torquer (MTQ) as the only actuator. Generally, in order to achieve high stabilization precision, in the satellite's attitude control systems (ACS) magneto-torquers are working together with other actuators, such as momentum or reaction wheels. The latter devices being costly and subject to failure, the advantages provided by the ACS without wheels are its cost-efficiency and reliability. Furthermore, after having been tested and proven effective, such PMC algorithm could be considered as a contingency ACS option of the magnetically controlled satellites.

Two approaches to the PMC design, namely *Linear Quadratic Regulator* (*LQR)* and *No Wheel* algorithms, are further set forth. According to the simulations, both of them can provide a good 3-axis stabilization of a satellite without the MW. Yet, as will be shown later, their implementation onboard the TechSat satellite is still a complicated problem.

2. LQR Controller [1]

2.1 Derivation of the control law

The dynamic system, represented by the satellite rotating under both control and environmental torques, can be described by the vector-matrix equation, as follows:

$$\dot{\bar{x}} = A\bar{x} + B\bar{u} + B_w\bar{w} \qquad (1)$$

$\bar{x}$ is the process state vector,

$$\bar{x} = \left(f, \dot{?}, ?, f, ?, ?\right) \qquad (2)$$

where, $f, ?, ?$ are Euler angles, that define the attitude of the satellite's Body Frame (BF) with respect to Trajectory Frame (TF) in the order $3 \rightarrow 1 \rightarrow 2$ rotation sequence, $\bar{u}$ is the control input, and $\bar{w}$ the process noise (disturbance vector).

This equation is generally nonlinear. It can be linearized, if the satellite's Body Frame (BF) rotation with respect to Trajectory Frame (TF) is slow enough.

In the specific case of magnetic control,

$$\bar{u} = \bar{m} \times \bar{b} \qquad (3)$$

with $\bar{m}$ =(m_x,m_y,m_z) - the magnetic control dipole moment, created by MTQ, and $\bar{b}$ =(b_x,b_y,b_z) - the environmental GMF vector along the satellite orbit.

For this case the dynamic system is defined by,

$$\begin{bmatrix} \dot{f} \\ \ddot{?} \\ \dot{?} \\ f \\ \dot{?} \\ ? \end{bmatrix} = \begin{bmatrix} 0 & 0 & w_0(1-s_1) & -4w_0^2 s_1 & 0 & 0 \\ 0 & 0 & 0 & 0 & 3w_0^2 s_2 & 0 \\ -w_0(1+s_3) & 0 & 0 & 0 & 0 & w_0^2 s_3 \\ 0 & 0 & 0 & 1 & 0 & 0 \\ 0 & 0 & 0 & 0 & 1 & 0 \\ 0 & 0 & 0 & 0 & 0 & 1 \end{bmatrix} \cdot \begin{bmatrix} f \\ \dot{?} \\ ? \\ f \\ ? \\ ? \end{bmatrix}$$

$$+ \begin{bmatrix} 0 & b_z(t)/I_{xx} & -b_y(t)/I_{xx} \\ -b_z(t)/I_{yy} & 0 & b_x(t)/I_{yy} \\ b_y(t)/I_{zz} & -b_x(t)/I_{zz} & 0 \\ 0 & 0 & 0 \\ & 0 & \\ 0 & 0 & 0 \end{bmatrix} \cdot \begin{bmatrix} m_1 \\ m_2 \\ m_3 \end{bmatrix} + \begin{bmatrix} 0 & 0 & 0 \\ 0 & 0 & 0 \\ 0 & 0 & 0 \\ 1/I_{xx} & 0 & 0 \\ 0 & 1/I_{yy} & 0 \\ 0 & 0 & 1/I_{zz} \end{bmatrix} \cdot \bar{n}_d \qquad (4)$$

Here,

w_0 - orbital mean motion,

I_{xx}, I_{yy}, I_{zz} - satellite principal moments of inertia,

s_1, s_2, s_3 - dimensionless moments of inertia:

$s_1 \equiv (I_{yy}-I_{zz})/I_{xx}$; $s_2 \equiv (I_{zz}-I_{xx})/I_{yy}$; $s_3 \equiv (I_{xx}-I_{yy})/I_{zz}$.

In (4), the BF axes are assumed to be collinear with principal axes of the satellite's ellipsoid of inertia. This assumption can be relaxed; in the latter case the involved matrices should include the effects of inertia products.

The linearized dynamical model, represented by (4), includes gravity-gradient, magnetic control, and disturbance torques. It can be re-written in the following form:

$$\dot{\bar{x}} = \tilde{A}\bar{x} + \tilde{B}(t)\bar{m} + B_w\bar{w} \qquad (4')$$

In Equation (4'), the only matrix depending on time is the control effectiveness matrix $\tilde{B}(t)$, its variations being caused by those of the GMF components. Moreover, the time variation of (4') can be approximated as periodic function, since $\bar{b}(t) \approx \bar{b}(t+T)$, where $T=2p/w_0$ is the orbital period, the major deviation from the strict periodicity being caused by the tilt of the geomagnetic dipole's axis from that of the Earth rotation.

The design of the control law, stabilizing the system (4'), was based on the periodic Linear Quadratic Regulator (LQR) technique [1,5]. The problem in question can be formulated as follows:

For $t \in [0, T]$, for the equation

$$\dot{\bar{x}} = \tilde{A}\bar{x} + \tilde{B}(t)\bar{m}$$

with $\bar{x}(0)$ given, find a linear control law

$$\bar{m}(t) = -K\bar{x}(t) \tag{5}$$

with gain matrix *K*, to minimize the cost function

$$J = \frac{1}{2}\int_0^T \left\{x^T(t)Qx(t) + m^T(t)Rm(t)\right\}dt + \frac{1}{2}x^T(T)P_T x(T) \tag{6}$$

where *Q* and *R* are constant matrices, and P_T is the terminal state weighting matrix. As known, the solution to this problem can be found in the form of a state-feedback control law:

$$\bar{m}(t) = -R^{-1}\tilde{B}^T(t)P(t)\bar{x}(t) \tag{7}$$

with *P(t)* being the solution to the time-dependent matrix Riccati equation. For P_T appropriately chosen, the resulting *P* would be periodic, with period *T*. This leads to a periodic gain,

$$K(t) = K(t+T) = -R^{-1}\tilde{B}^T(t)P(t) \tag{8}$$

In case of the magnetic attitude control, it is better to express the gain in the form (8), instead of computing its time history. What's more, in the control effectiveness matrix $\tilde{B}(t)$ of (4'), the MGM measurements can be substituted, to make the computed gain compensated for the uncertainties in the GMF model.

In case *P(t)* is a constant matrix: $P(t)=P_{ss}$, the control law (7) would be even more simple for use in a real system, without the need to keep the whole matrix time history. Furthermore, a constant P_{ss} would not need to have its time variations synchronized with the actual time variations in $\tilde{B}(t)$.

Once calculated, the P_{ss} matrix can be used in the control law

$$\begin{aligned} &\bar{m} = -K\bar{x} \quad \text{, where} \\ &K = -R^{-1}\tilde{B}^T(t)P_{ss} \end{aligned} \tag{9}$$

To eliminate the steady-state effects of the disturbances, the enlarged state vector $\bar{x}_{aug} = [\bar{z}, \bar{x}]$ was introduced instead of $\bar{x}$, with $\bar{z}$ being a 3×1 vector of integrals of the attitude errors:

$$z_i(t) = \int_0^t x_i(t)dt \ , \quad i = 1,2,3 . \tag{10}$$

Then the augmented model equation will acquire the following form,

$$\dot{\bar{x}}_{aug} = \begin{bmatrix} 0 & [I_{3\times3}, 0 \\ 0 & \tilde{\tilde{A}} \end{bmatrix} \bar{x}_{aug} + \begin{bmatrix} 0 \\ \tilde{\tilde{B}}(t) \end{bmatrix} \bar{m} + \begin{bmatrix} 0 \\ B_w \end{bmatrix} \bar{w} \qquad (11)$$

with matrices $\tilde{\tilde{A}}, \tilde{\tilde{B}}(t)$, and B_w the same as in (4').

2.2 Control implementation by PWM technique

Each one of the three TechSat MTQ dipoles can have one of three possible values of magnetic moment:

$$M_{sat},\ 0,\ -M_{sat} \qquad (12)$$

where $M_{sat} \approx 1 \text{Amp}\cdot\text{m}^2$ is the MTQ dipole saturation value. The total number of feasible standard dipole combinations (vectors) for 3-axis MTQ is thus equal to 26.

Furthermore, to prevent the distortion of MGM measurements by MTQ functioning, magnetic field measurements and MTQ actuation are separated in time. Within each second, 0.3 seconds are allotted for measurements, and the rest for control.

In order to adequately approximate the required control dipole moment $\bar{m}$ by the permissible MTQ dipole moments (12), a PWM technique is applied. According to it, the dipole moment, to be created by the MTQ, is kept constant during the whole *controller decision cycle*, e.g. one minute. Once per minute, a table of 600 lines and 3 columns is filled out, each line containing a set of 3 standard dipole moments for every tenth of a second. This table should be built up so as the *actual* dipole moment created by the MTQ during a minute to be as close as possible to the *required* one.

Example 1. If $m(1)$ = 0.027 Amp·m^2, then the contents of the table's 1st column are set as follows:

Time (s)	m(1)
0.1	1
0.2	1
0.3	1
0.4	1
0.5	1
0.6	1
0.7	1
0.8	0
0.9	0
1.0	0
1.1	1
1.2	1
1.3	1
1.4	1
1.5	1
1.6	1
1.7	1
1.8	0
1.9	0
2.0	0
2.1	1
2.2	1
2.3	0
…	0
60.0	0

So the actual dipole moment will be

$m(1)=16/600=0.026666$ Amp·m^2 .

After a number of simulations, three improvements were added to this algorithm:

1. It is not recommended to have MTQ working during a too large part of a minute, to prevent an excessive change of the satellite attitude, before the next decision would be taken, and the new cycle would start.

Example 2: Let the required dipole moment $\overline{m}$ be (0.5, 0, 0). According to aforesaid, an x-axis MTQ dipole should be actuated for 30 seconds within a given minute. Still, after having this done, the resulting change of the angular velocity would be

$$\Delta\overline{w} = \frac{\overline{u}}{I}dt = \frac{(\overline{m}\times\overline{B})}{I}dt \approx \frac{(\tilde{\overline{m}}\times\overline{B})}{I}dt = \frac{\left|\tilde{\overline{m}}\right|\cdot\left|\overline{B}\right|}{I}dt = 0.005\sec^{-1}$$

where

$$\left|\tilde{\overline{m}}\right| = 1Amp\cdot m^2$$
$$\left|\overline{B}\right| = 2.5\cdot 10^{-5}Tesla$$
$$dt = 30^{s}$$
$$I = 1.5kg\cdot m^2$$

To prevent such an effect, a limitation was imposed on the possible number of seconds the dipoles can be turned on. This number - T_{max} - was chosen equal to 10^s for the x- and z-axis dipoles, and to 30^s for the y-axis dipole. This automatically limits the maximum value of the control dipole, obtainable within a minute (saturation value):

$$\overline{U}_{\max} = \frac{\overline{T}_{\max}\cdot t_{in}\cdot 1Amp\cdot m^2}{t_{pwm}} = [0.1167,\ \ 0.3500,\ \ 0.1167]Amp\cdot m^2$$

where

t_{in} = $0^s.7$- part of a second eligible for control,

t_{pwm} = 60^s - controller decision cycle.

2. In case if, due to the saturation, any of the required dipoles gets larger than corresponding $\overline{U}_{\max}$ component, $\overline{m}$ is changed as follows:

For x- or z-axis dipoles:

$m(1) = C\cdot m(1)$,

$m(3) = C\cdot m(3)$,

where

$$C = \max\left(\frac{|m(1)|}{U_{\max}(1)}, \frac{|m(3)|}{U_{\max}(3)}\right)$$

For y-axis dipole:

$m(2) = \text{sign}(m(2))\cdot U_{max}(2)$.

3. Additional fine-tuning of the control can be achieved by calculating the difference between $\overline{m}$, and the actual MTQ dipole moment $\tilde{\overline{m}}$, and adding it to $\overline{m}$, as required for the next minute.

Example 3. Let *m*(i) required at the n^{th} minute be equal to 0.0355Amp·m^2. Turn on the i-axis dipole for 3 seconds, during 0.7^s in each second, to get

$\tilde{m}(i)$ = (3·0.7)/60 = 0.035 Amp·m^2

The difference *m*(i)- $\tilde{m}(i)$ =0.0005 Amp·m^2 is to be added to *m*(2) required for the (*n+1)*-st minute.

2.3 Simulation Results

The implementation of the control law (7) assumes a full-state feedback, that can be provided by the Kalman filter. Matrix $\tilde{A}$ in (4,4') being constant, the state transition matrix $F = \exp(\tilde{A} \cdot dt)$, with *dt* given, would be constant as well, enabling thus the application of the Linear Kalman Filter (LKF).

While adjusting LKF to the LQR controller, it was taken into account, that the TechSat onboard computer (OC) is unable to support implementation of a standard Kalman filter's algorithmic sequence [6], that implies, specifically, the whole measurement update phase to be carried out at the times the measurements are referred to. Due to the excessive time required by OC, this phase was split into 12 parts, each of them to be executed piecemeal, once in 12^s. The MGM measurements' sampling time was thus also 12^s.

In Graphs 1-6, the LQR performance is shown, with MW fixed, its angular momentum H_w being thus zero. In this case, the satellite's BF axes are assumed to coincide with the principal axes of its inertia ellipsoid. The initial conditions for the *Truth model*, and the dynamical parameters of the satellite are as follows:

f	0.0001 rad/s
$\dot{?}$	-0.001 rad/s
$?$	0.0001 rad/s
j	12º.9
q	3º.5
y	11º.9
H_w	0
I_{xx}	1.754 kg.m^2

I_{yy}	1.677 kg.m^2
I_{zz}	1.696 kg.m^2

The state vector components in the *Truth model* are plotted in black, while those of the LKF estimate in red.

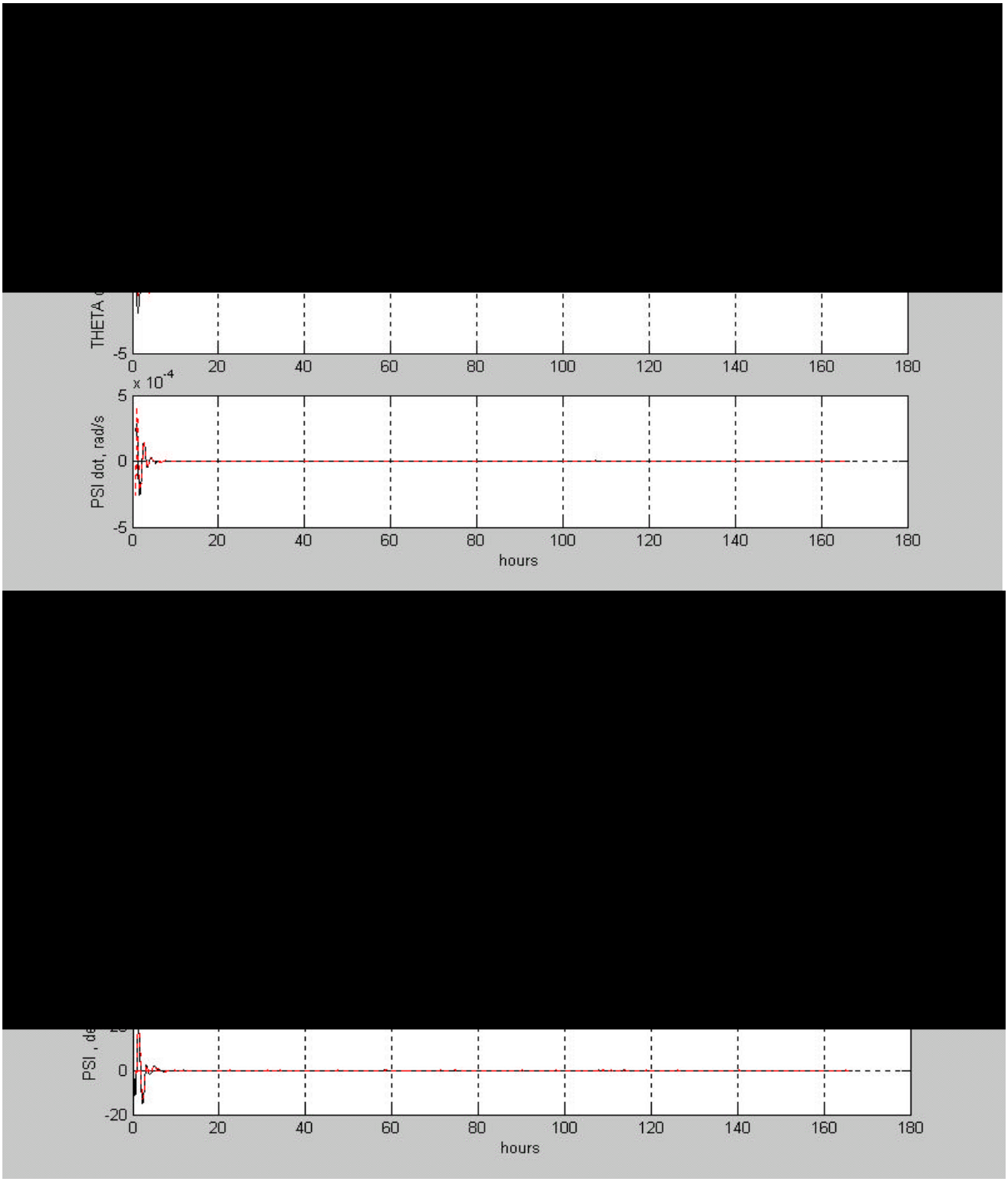

In the next simulation, represented by Graphs 7-12, non-diagonal tensor of inertia is involved both in the *Truth model* and in LKF, with inertia products equal to:

I_{xy}	0.015 kg.m^2
I_{xz}	0.070 kg.m^2
I_{yz}	0.044 kg.m^2

The $\tilde{A}$ matrix now being

$$\tilde{A} = I^{-1} \cdot \begin{bmatrix} 0 & -2I_{yz}\, w_0 & (I_{zz} - I_{yy} + I_{xx})\, w_0 \\ 2I_{yz}\, w_0 & 0 & -2I_{xz}\, w_0 \\ (I_{yy} - I_{xx} - I_{zz})\, w_0 & 2I_{xy}\, w_0 & 0 \\ 0 & 0 & 0 \\ 0 & 0 & 0 \\ 0 & 0 & 0 \end{bmatrix} \begin{bmatrix} 4(I_{zz} - I_{yy})\, w_0{}^2 & -3I_{xy}\, w_0{}^2 & I_{xz}\, w_0{}^2 \\ -4I_{xy}\, w_0{}^2 & 3(I_{zz} - I_{xx})\, w_0{}^2 & -I_{yz}\, w_0{}^2 \\ 4I_{xz}\, w_0{}^2 & 3I_{yz}\, w_0{}^2 & (I_{xx} - I_{yy})\, w_0{}^2 \\ 1 & 0 & 0 \\ 0 & 1 & 0 \\ 0 & 0 & 1 \end{bmatrix} \tag{13}$$

where I^{-1} is the inverse of the inertia tensor.

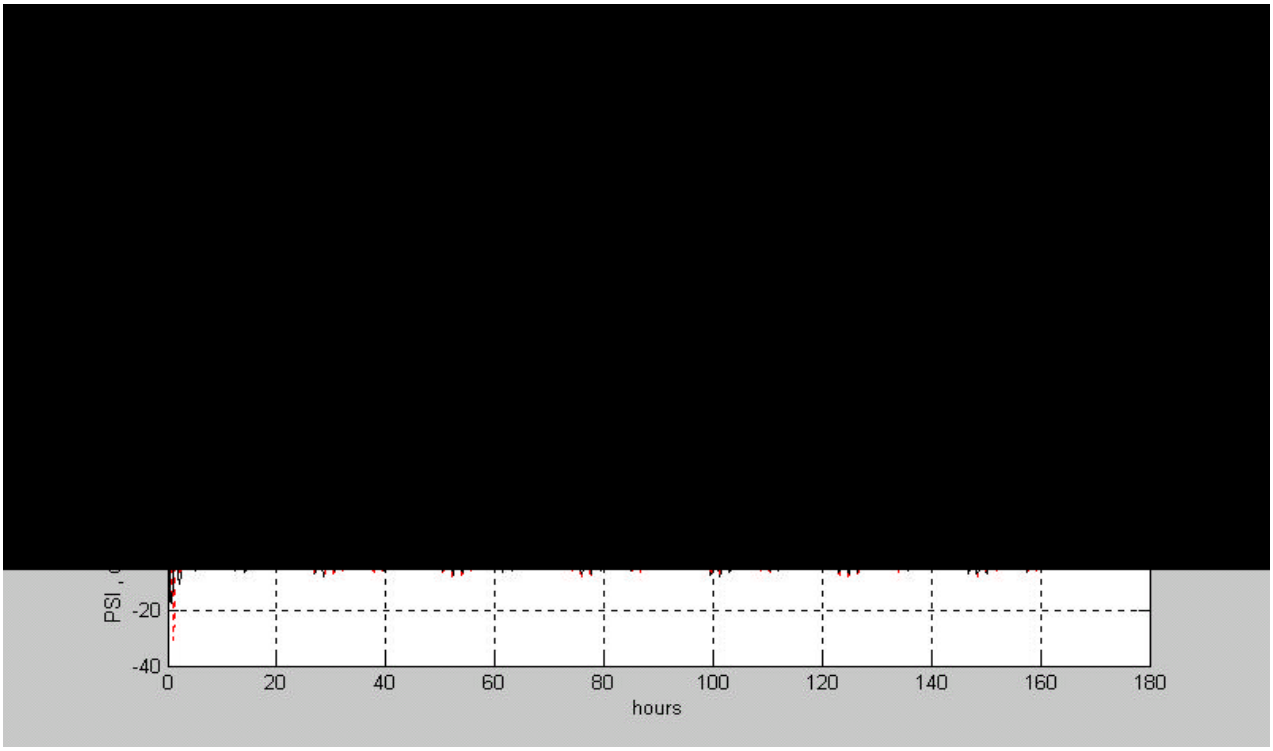
-20
-40
0
20
40
60
80
100
120
140
160
180
hours

2.4 Planning the Flight Experiment

Nominally, the TechSat satellite's attitude is controlled by concerted functioning of its 3-axis MGM, 3-axis MTQ, and the momentum wheel (MW), the latter providing the satellite's stability and also implementing the pitch control. The nominal MW momentum bias is about -0.42 Nt·m·s. To provide 3-axis stabilization of the TechSat under these operation conditions, the proportion-plus-derivative *COMPASS* control law [3] is applied once per second:

$$\vec{M} = -K \cdot (\dot{\vec{B}}_{meas} - \dot{\vec{B}}_{\exp}) + C \cdot (\vec{B}_{meas} - \vec{B}_{\exp}) \qquad (14)$$

where $\vec{M}$ - control magnetic moment of MTQ,

$\vec{B}_{meas}, \dot{\vec{B}}_{meas}$ - measured GMF vector and its derivative, as referred to the Body Frame (BF),

$\vec{B}_{exp}, \dot{\vec{B}}_{exp}$ - expected GMF vector and its derivative, as referred to the Trajectory Frame (TF),

Therefore, in order to test the *LQR* algorithm, included in the testing sequence should be the phase of slowing down and stopping the wheel. It should be clear, that this operation would bring about the destabilization of the satellite, before the control algorithm gets actuated.

Some remarks are to be made, while choosing the test sequence, viz.:

1. As a result of slowing down and stopping the MW, the satellite gets destabilized, and starts to tumble;
2. Since LQR controller can be actuated only after LKF initialization, a slow enough satellite's rotation is assumed here.

The graphs 13-19 display the simulation according to the scenario as follows:

a. Initially, the satellite is 3-axis stabilized, *COMPASS*-controlled, with *Hw* nominal;
b. While keeping the *COMPASS* control on, the wheel is gradually slowed down to the angular momentum $Hw \approx -0.005$ Nt·m·s within $\approx 11^h$;
c. At $T \approx 11^h$, LKF gets initialized;
d. d. At $T \approx 27^h.8$, *LQR* controller is actuated.

The matrix $\tilde{A}$ in (13) was appropriately modified, to take into account non-zero *Hw*.

As can be seen in the Graphs, the COMPASS control provides acceptable 3-axis stabilization even with *Hw* as small as –0.005 Nt·m·s. After switching to *LQR*, the attitude converges to the steady-state oscillations similar to those in Graphs 10-12.

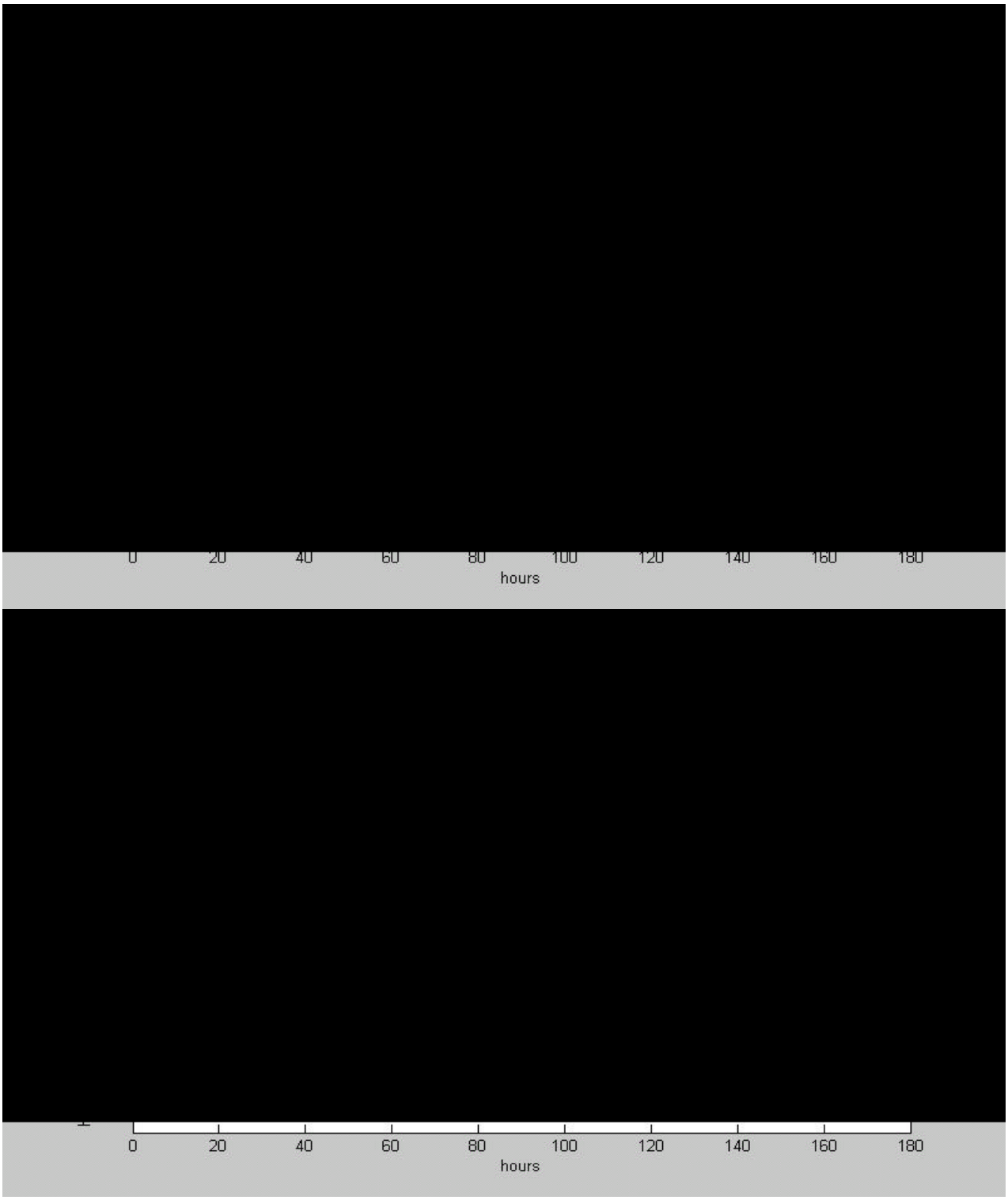
0
20
40
60
80
100
120
140
160
180
hours
0
20
40
60
80
100
120
140
160
180
hours

2.5 Flight Experiments

a. The 1st flight experiment consisted in slowing down the MW under *COMPASS* control to angular momentum of –0.05 Nt·m·s. The MGM telemetry and the results of its processing are displayed in Graphs 20 – 30.

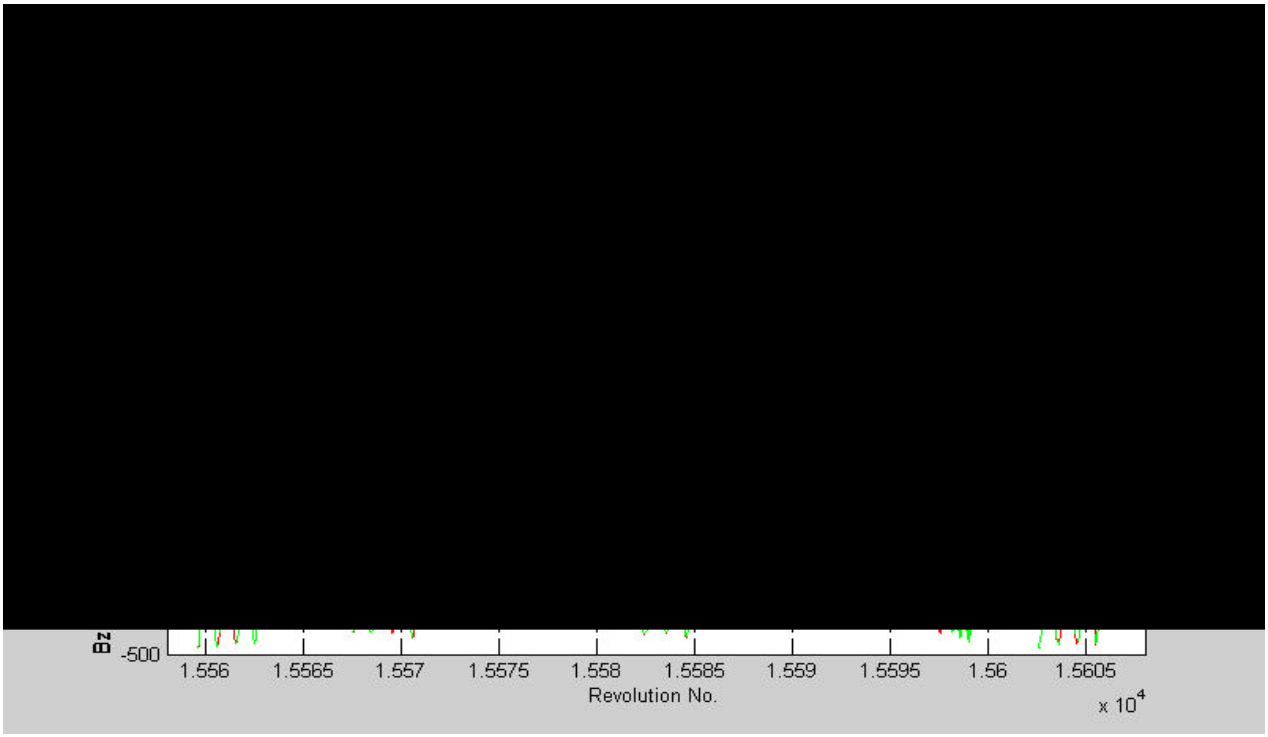

The MW angular momentum before and during the experiment is shown in Graph 20. In the Graphs 21-23, the expected values (GMF model), calculated with IGRF2000 model and SGP4 orbital predictor [3], are plotted in green, while MGM telemetry – in red.

As seen, before the experiment the measurements match well with the GMF model. Although referred to 2 different reference frames, TF and BF, respectively, their closeness evidences good 3-axis stabilization of TechSat by the *COMPASS* control. During the MW deceleration, the satellite gets destabilized, and later on, by the same control, resumes stabilization. Graphs 24-30 show the TechSat attitude as estimated by the Extended Kalman Filter (EKF) of the Ground Estimator (GE) [3]. The GE state vector includes:

w_x, w_y, w_z - Components of the instantaneous angular velocity of the Body Frame (BF) with respect to Inertial Frame (IF), as referred to BF axes;

j, q, y - Euler angles, defining the attitude of the BF with respect to Trajectory Frame (TF) in the order $3 \rightarrow 1 \rightarrow 2$ rotation sequence;

b_x, b_y, b_z - components of the MGM bias with respect to BF .


x 10

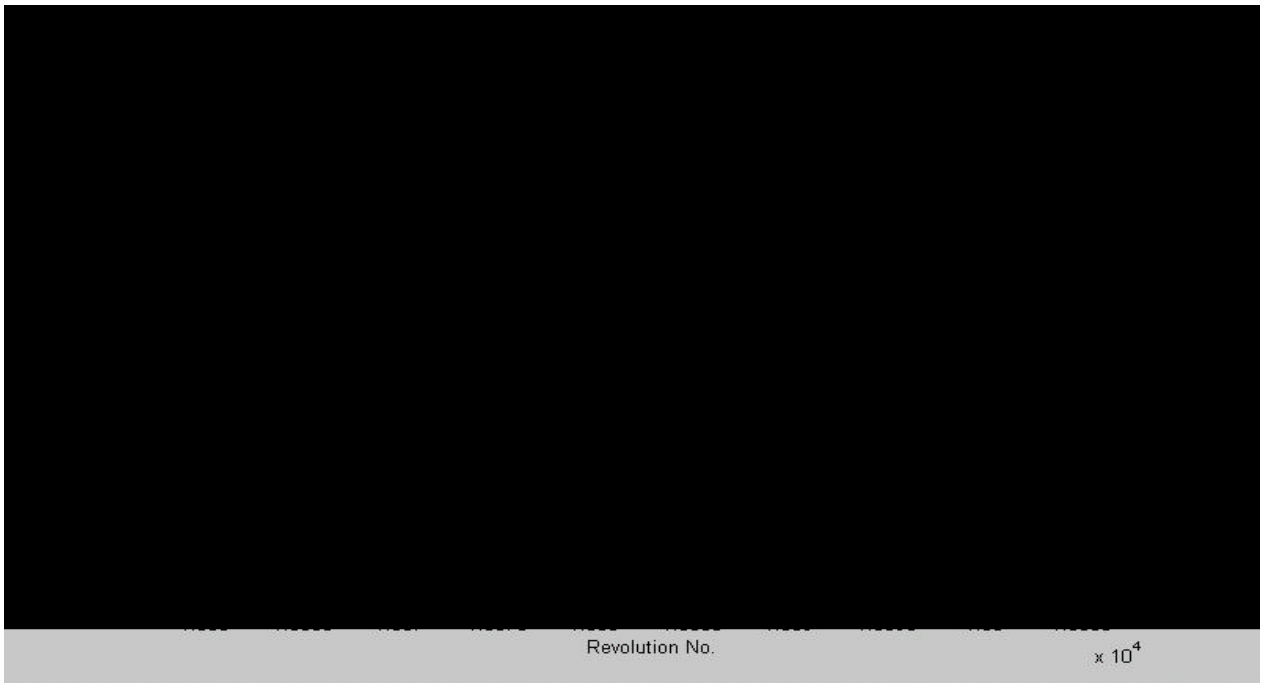
Revolution No.
x 10^4

b. The 2nd flight experiment consisted in slowing down the MW from – 0.01Nt·m·s to –0.001Nt·m·s under the *COMPASS* control, and testing the onboard LKF. The comparison of the measured GMF components with expected ones, as seen in the graphs 32-34, displays no perturbations that could testify a destabilization, the maximum differences between the Y-axis components amounting to as much as 30 to 40 mGAUSS, while those in X-and Z-axes never exceeding 5-7 mGAUSS. But anyway, throughout the experiment, the MGM measurements keep in a good correspondence with the GMF model, both in phase and in amplitude. Another evidence of the attitude smoothness while the MW deceleration is the state vector estimates (graphs 35-40), as made by GE (in black) and the onboard LKF (in red). Their patterns differ mainly because of the different abundance of the measurements involved in the processing.

   The conclusion to be made here is that the TechSat didn't get destabilized while slowing down the MW. Yet without the independent checking, based on a sensor other than MGM, this couldn't be confirmed. As known, the only sensor fit for such a checking is the onboard camera; but its performance became problematic, and failed in all the attempts during the experiment in question.

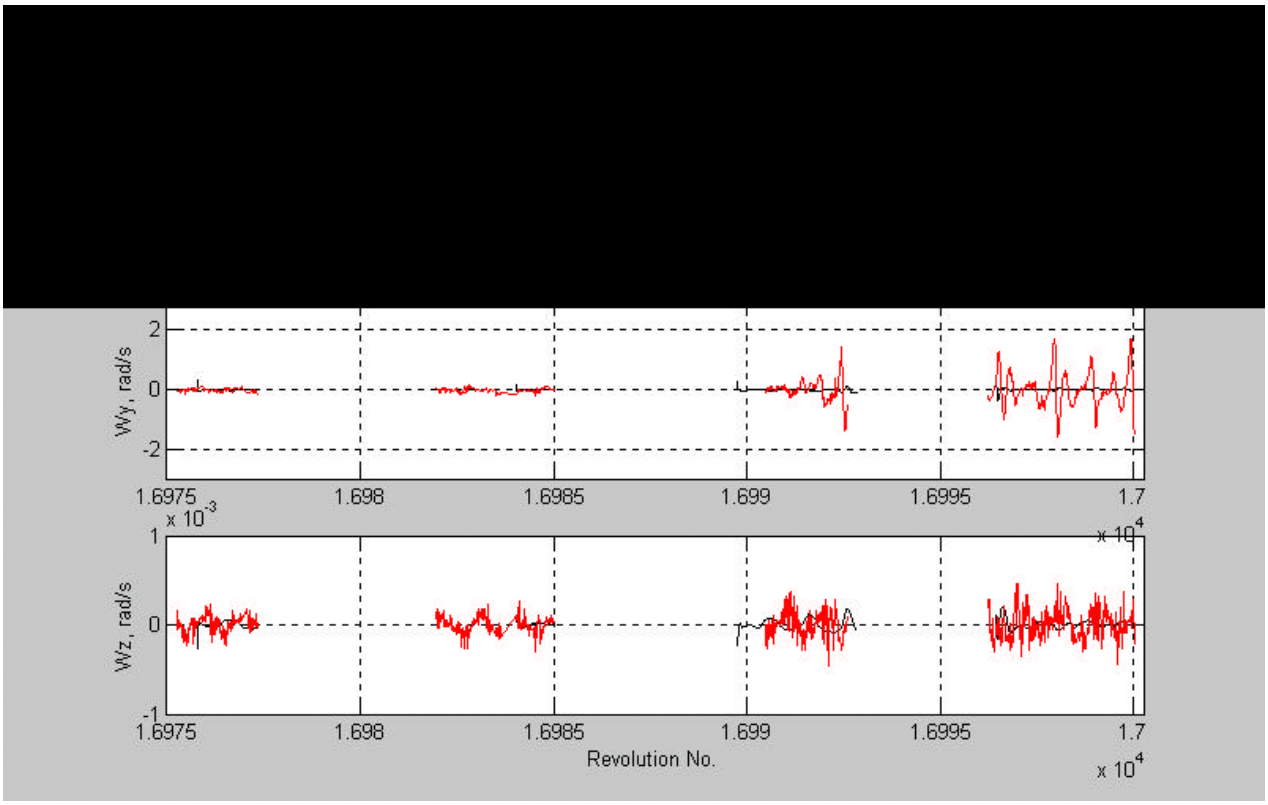
Wy, rad/s
2
0
-2
1.6975
1.698
1.6985
1.699
1.6995
1.7
x 10^-3
x 10^4
Wz, rad/s
1
0
-1
Revolution No.
x 10^4

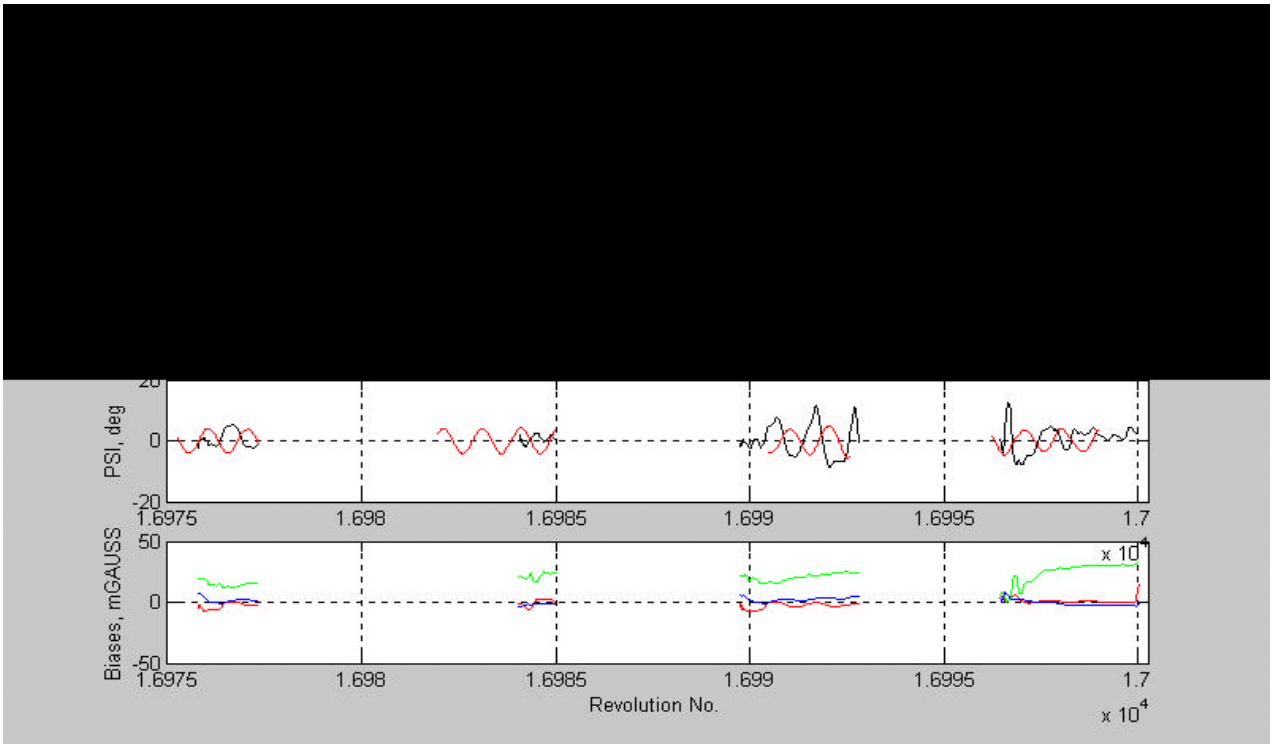
PSI, deg
0
-20
1.6975
1.698
1.6985
1.699
1.6995
1.7
Biases, mGAUSS
50
0
-50
x 10^4
Revolution No.
x 10^4

Another conclusion is that during the MW's slowing down, its coil was creating an additional magnetic dipole moment along the BF Y-axis that disturbed the respective component of the MGM measurements.

c. The 3rd flight experiment consisted in stopping the MW, its initial Hw being –0.001Nt·m·s. When comparing the MGM measurements with the GMF model (graphs 43,44,45), they seem to keep the conformity both in the amplitude and in the phase, as in the previous experiment. But now one prominent distinction with the latter case can be seen, viz: the spike-shaped perturbations in the measured B_y, that sometimes amount to 100 mGAUSS, and even more. Here again, there was no possibility for independent checking of this, seemingly, 3-axis stabilized attitude with the onboard camera.

Seen is also, that the onboard LKF estimates exceed the limits the linear model can afford.

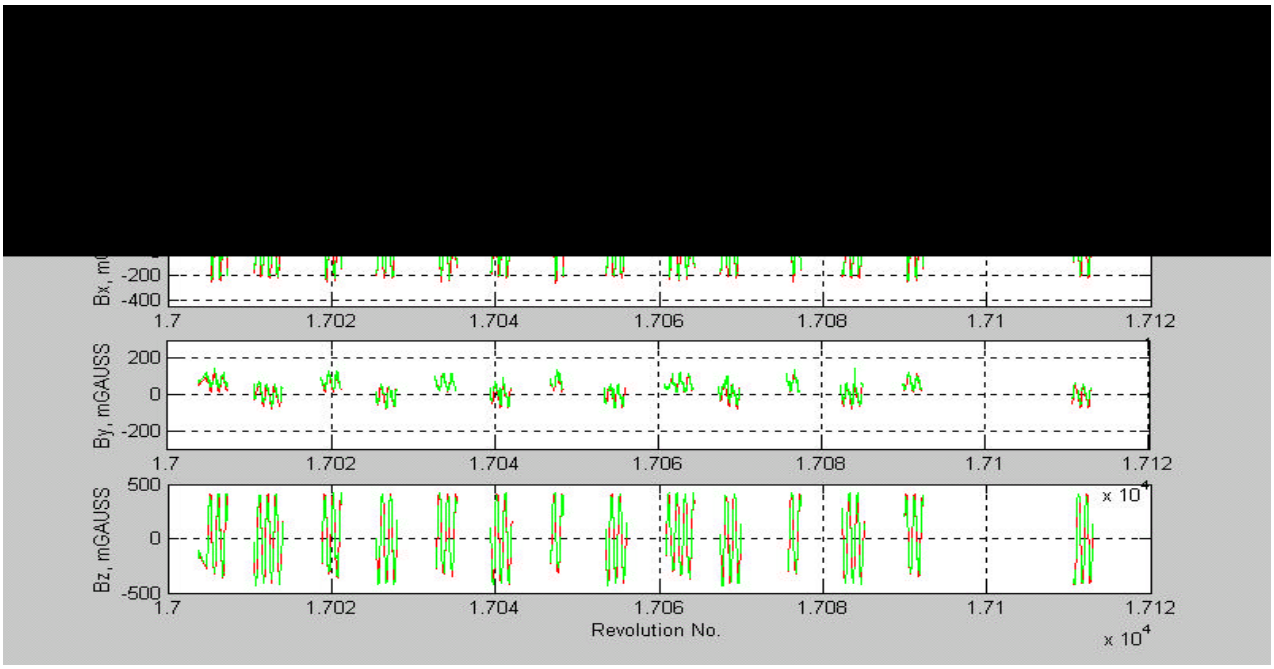

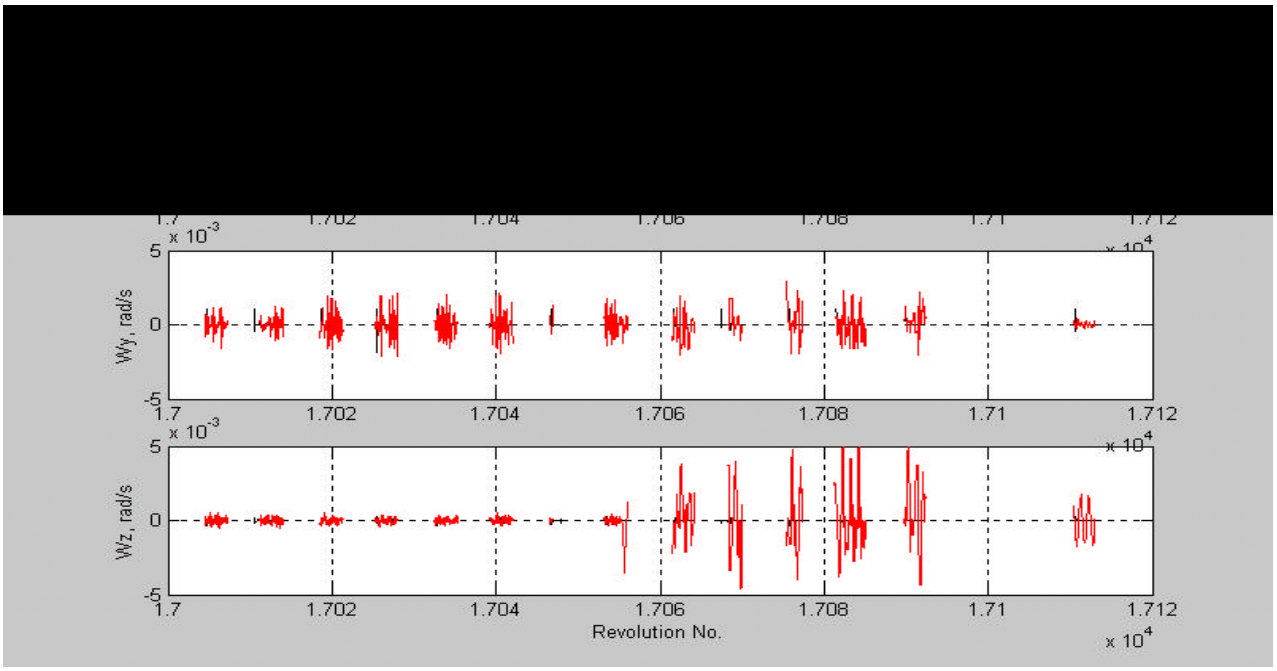
x 10^-3
5
0
-5
Wy, rad/s
1.7
1.702
1.704
1.706
1.708
1.71
1.712
x 10^4
Wz, rad/s
Revolution No.

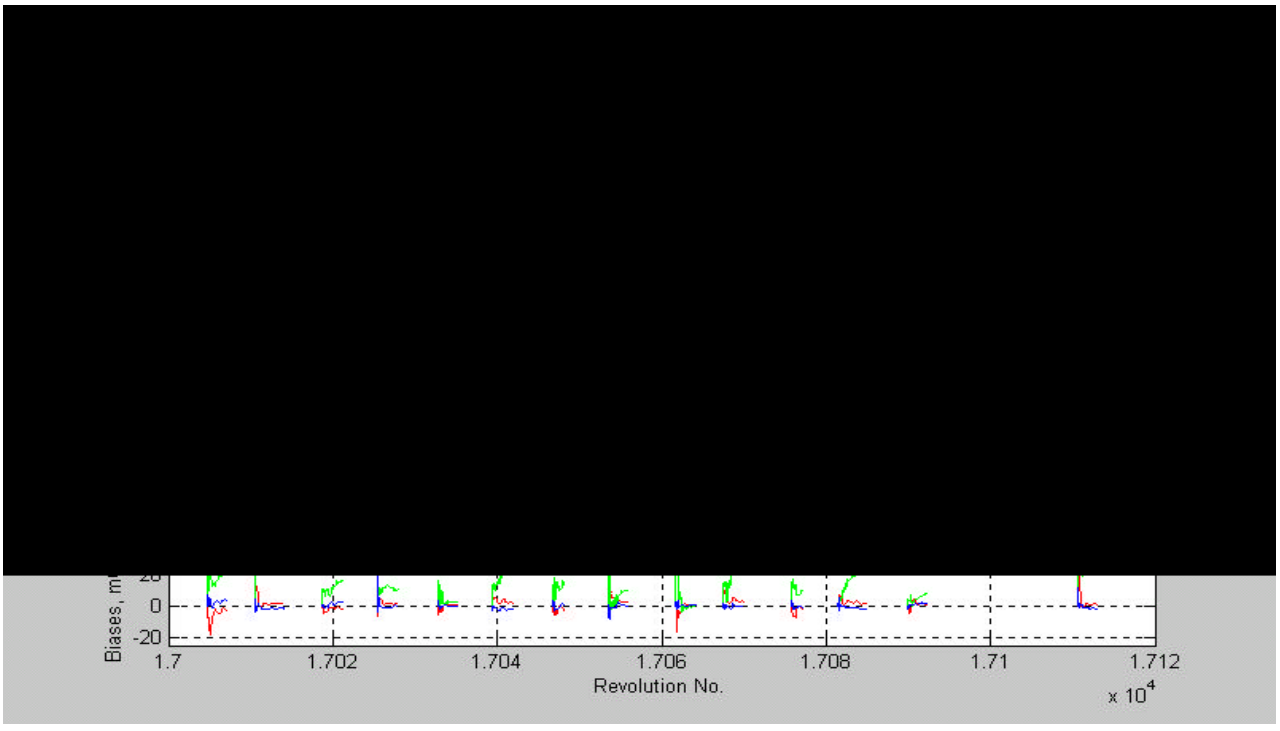
Biases, m
0
-20
1.7
1.702
1.704
1.706
1.708
1.71
1.712
Revolution No.
x 10^4

3. "NO_WHEEL" Algorithm

3.1 Analytical expression of the *No Wheel* control law

The control torque $\bar{T}$, to provide the satellite's stabilization without momentum wheel, can be expressed as follows [2]:

$$\begin{aligned} T_x &= -(C_1 ?'_x + C_2 q_x / I_{xx}) \\ T_y &= -(C_1 ?'_y + C_2 q_y / I_{yy}) \\ T_z &= -(C_1 ?'_z + C_2 q_z / I_{zz}) \end{aligned} \qquad (15)$$

where:

$\vec{w}'(w'_x, w'_y, w'_z)$ - Instantaneous angular velocity of the Body Frame (BF) with respect to the Trajectory Frame (TF), as referred to BF axes;

q_x, q_y, q_z - Quaternion components (Euler symmetric parameters) of the BF attitude with respect to TF;

C_1, C_2 - Control gains.

Still the *required* torque (15) cannot be applied to the satellite directly, since, physically, the magnetic control torque is implemented as a cross-product of the relevant magnetic moment $\bar{m}$ built up by the MTQ, and the environmental GMF vector $\bar{B}$:

$$\bar{U} = \bar{m} \times \bar{B} \qquad (16)$$

In the *"No Wheel"* algorithm, the magnetic moment $\bar{m}$ is calculated as,

$$\bar{m} = \frac{\bar{B} \times \bar{T}}{|\bar{B}|^2} \qquad (17)$$

where $\bar{T} = (T_x, T_y, T_z)$.

According to (2), vectors $\bar{U}$, $\bar{T}$, and $\bar{B}$ would always be coplanar (see Fig.1):

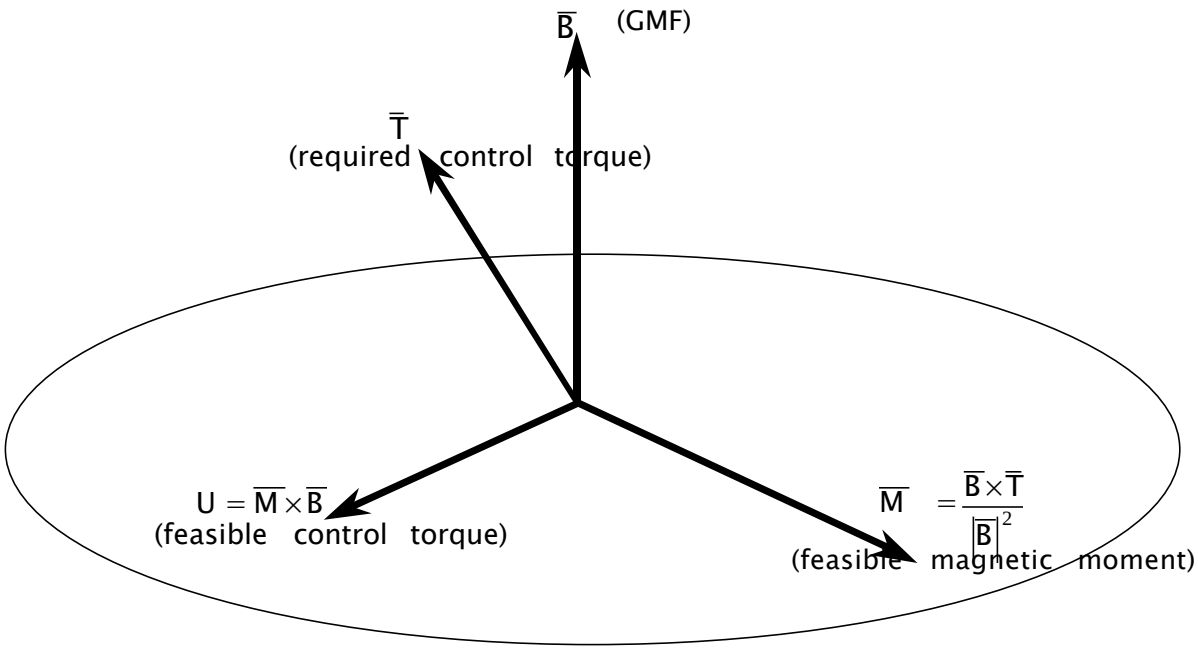

Fig. 1: Magnetic control vector definitions

3.2. Implementing the *No Wheel* control law

The technique of the *No Wheel* implementation, in many respects, is similar to the PWM one, as described in paragraph 2.2, with some differences. Now the table to be filled out, contains 100×10 lines and 3 columns, its size always being kept constant. At the same time, the *controller decision cycle*, or the time interval between two successive table fill-outs, typically equal to 100 seconds, can be shortened, when the satellite's attitude changes fast or, equivalently, when the required control dipole moment, which is calculated each second, gets "too large". The latter criterion is a matter of trial-and-error choice.

4. Extended Kalman Filter for Attitude Determination

The inputs to the PMC controller are the satellite's attitude parameters, to be estimated from the MGM measurements by the Extended Kalman Filter (EKF). As known [6], the algorithmic sequence in the EKF has the following steps:

4.1 Time Update

1. Given the satellite's attitude state vector estimate X_k at the moment t_k, propagate it to the moment t_{k+1}, by integrating Euler kinematic and dynamical equations:

$$X_k(+) \rightarrow X_{k+1}(-) \tag{18}$$

where (-) and (+) refer to *a priori* and *a posteriori* estimates, respectively;

2. Propagate the state covariance matrix:

$$P_{k+1}(-) = F\, P_k(+)\, F^T + Q \tag{19}$$

where F is the state transition matrix at t_k, and Q is the process noise covariance matrix.

4.2 Measurement Update

1. Calculate the Kalman gain matrix:

$$K_{k+1} = P_{k+1}(-)\, H^T\, [H\, P_{k+1}(-) H^T + R\,]^{-1} \tag{20}$$

where H is the measurement matrix, and R is the measurement noise matrix.

2. Calculate the state vector error at t_{k+1}:

$$dX_{k+1} = K_{k+1}\, [z_{k+1} - H\, X_{k+1}(-)] \tag{21}$$

where z_{k+1} is the measurement vector;

3. Update the state vector at t_{k+1}, to obtain its *a posteriori* estimate:

$$X_{k+1}(-),\, dX_{k+1} \rightarrow X_{k+1}(+) \tag{22}$$

4. Update the state covariance matrix at t_{k+1}:

$$P_{k+1}(+) = [I - K_{k+1}\, H]\, P_{k+1}(-)\, [I - K_{k+1} H]^T + K_{k+1}\, R\, K^T_{k+1} \tag{23}$$

To be fit to any attitude kinematics, including the fast rotation, the time propagation has to be carried out with small enough step size (0.1^s, or so). Furthermore, the whole measurement update phase has to be fulfilled at the times the measurements are taken.

As verified in numerous simulations, PMC *No Wheel* algorithm, based on the control law (15, 17) with compensation for the steady-state errors, and fed by such a generic EKF, enables a 3-axis stabilization within $\pm 5^o$ under any initial conditions, no matter how the transition is carried out from the nominal control to *No Wheel* control.

5. EKF TechSat Implementation

As in the case with LKF, the TechSat onboard computer (OC) is unable to support a standard implementation of the EKF algorithm. To install the EKF algorithm in the TechSat OC, EKF elements were properly modified, to adjust it to the computer capacity at a cost of the universality of the EKF. This modification includes:

a. An increase of the step size to 1^s,
b. Splitting the whole measurement update phase into 10 parts, each part being executed once in 10^s.

In order to let such a constrained EKF keep pace with the satellite's kinematics, the satellite attitude dynamics has to be slowed down, and to be henceforth carefully controlled. Once-per-10^s control was experimentally found to be a good choice.

The state vector to be estimated by both the onboard and Ground Station (GS) EKFs, was chosen as follows:

w_x , w_y , w_z - Components of the instantaneous angular velocity of the Body Frame (BF) with respect to Inertial Frame (IF), as referred to BF axes;

j , q, y - Euler angles, defining the attitude of the BF with respect to Trajectory Frame (TF) in the order $3 \rightarrow 1 \rightarrow 2$ rotation sequence;

b_x , b_y , b_z - components of the MGM bias with respect to BF .

6. Planning the Experiment

The principal considerations to be taken into account, while choosing the test sequence, are similar to those in paragraph 2.4:

a. As a result of slowing down and stopping the MW, the satellite gets destabilized, and starts twisting;
b. PMC controller can be actuated only after EKF initialization;

c. The modified EKF can converge only in a slow motion case.

As was found out from the simulations, there can be two possible scenarios of switching from nominal control with MW rotating, to *No Wheel* control, that comply with these considerations.

6.1 Scenario A

A.1 Initially, the satellite is 3-axis stabilized under the once-per-sec nominal *COMPASS* control law. The MW is assumed to maintain the nominal angular momentum

$$Hw \approx -0.42\ Nt{\cdot}m{\cdot}s$$

A.2. Slow down MW, while applying the *COMPASS* control at a once-per-sec rate;

A.3. When $Hw \approx -0.001$ Nt·m·s, stop MW and turn off the control, thus bringing the satellite into *torque-free rotation* (tumbling);

A.4. Initialize EKF, and run it for a sufficiently long period, still holding on the *torque-free rotation*;

A.5. Turn on the *No Wheel* algorithm.

6.2 Scenario B

B.1 and B.2 stages are the same as A.1 and A.2 ones.

B.3. Slow MW down to zero; when *Hw* is about –0.005 Nt·m·s, switch *COMPASS* control over from once-per-1^s to once-per-10^s rate.

B.4. Initialize EKF, and run it for a sufficiently long period, while keeping once-per-10^s *COMPASS* control.

B.5. Turn off MW, and turn on the *No Wheel* algorithm

7. Simulation Results

7.1. *Scenario A* simulation

An example of the attitude control simulation according to *Scenario A* is represented in the graphs 53-59, truth model plots being plotted in black, while those of the modified EKF – in red. The initial conditions were as follows:

w_x	-0.0016 rad/s
w_y	-0.0002 rad/s
w_z	-0.0023 rad/s
j	-40º.9

q	-27º.0
y	-32º.7
H_w	-0.4178 Nt·m·s

The satellite is assumed to have its BF axes collinear with principal axes of its inertia ellipsoid, its principal moments of inertia being

I_{xx} - 1.754 kg.m^2

I_{yy} - 1.677 kg.m^2

I_{zz} - 1.696 kg.m^2

In the satellite's dynamics, along with the control torque, the gravity gradient torque was also taken into account. The control sequence included:

1. *COMPASS* control phase: $0^h \div 67^h$, with the simultaneous momentum wheel's slowing down from H_w nominal to –0.0006 Nt.m.s;
2. *Control Torque-free* phase: $67^h \div 78^h$, with stopping the wheel and EKF initialization;
3. *No wheel* control phase: $78^h \div 305^h$.

The main results displayed in the graphs are:

The satellite can keep 3-axis stabilization under *COMPASS* control even with a very low H_w of about –0.005 Nt.m.s.

The angular velocity components w_x and w_z, reduced to 0.0003-0.0005 rad/s level by the *COMPASS* control, do not vary substantially after the MW is stopped; this is an important condition for EKF adequate performance; at the same time w_y can become twice, or even trice as much.

The smallness of w_x and w_z provides moderate variation of j and y angles, which guarantees the convergence of the *No Wheel* control.

It takes the satellite about 30^h (≈20 revolutions) to get coarsely 3-axis stabilized, and about twice as much – to achieve the steady state, with the amplitudes in j, q, y of about 5º.

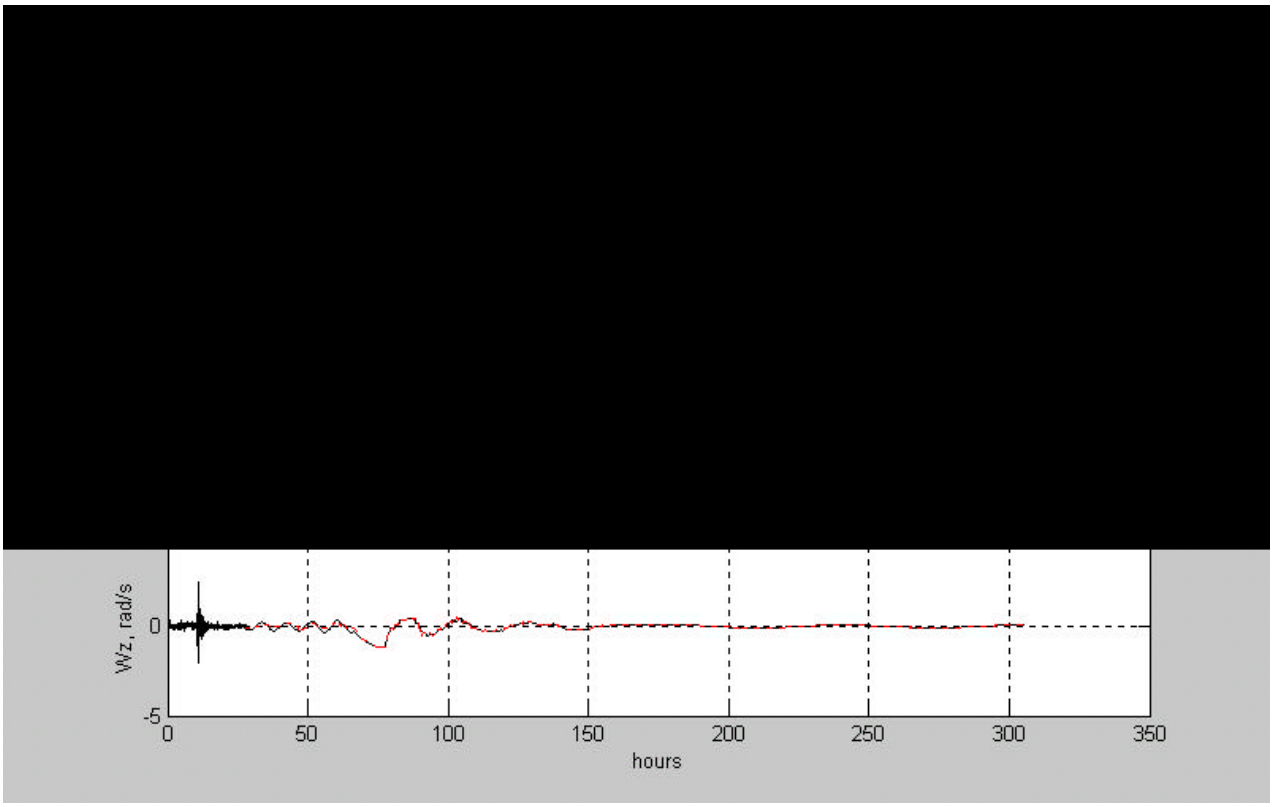
Wz, rad/s
0
-5
0
50
100
150
200
250
300
350
hours

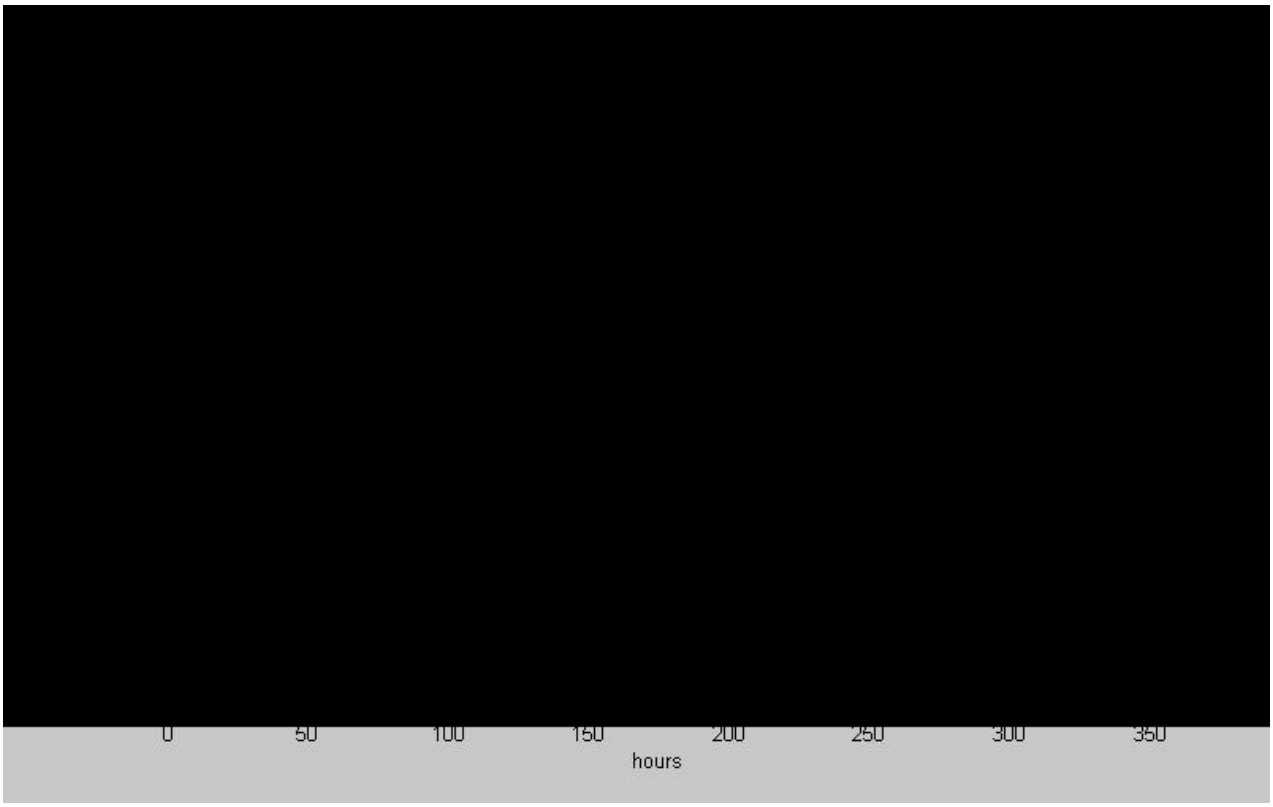
0
50
100
150
200
250
300
350
hours

7.2. Scenario B Simulation

The control sequence included:

1. *COMPASS* control phase: $0^h \div 78^h$, with H_w damping down from the nominal value to $\approx$–0.0006 Nt·m·s, and EKF initialization;

2. *No wheel* control phase: $78^h \div 305^h$, with stopping MW.

The results obtained in the simulation according to *Scenario B*, are shown in Graphs 60-66. The initial conditions were the same as in the *Scenario A* simulation.

The main difference between the two simulations consists in a more restrained variation of w_x and w_z, and hence of j and y, during the direct transition from *COMPASS* to *No Wheel* control in the *Scenario B*, so that the satellite could even keep the 1-axis stabilization during this period of time. The w_y component, meanwhile, gains in the *Torque-free* phase as much as 5 times. As for the performance of the *No Wheel* algorithm, the convergence process looks similar in both scenarios, and takes approximately equal time, to achieve steady-state stabilization.

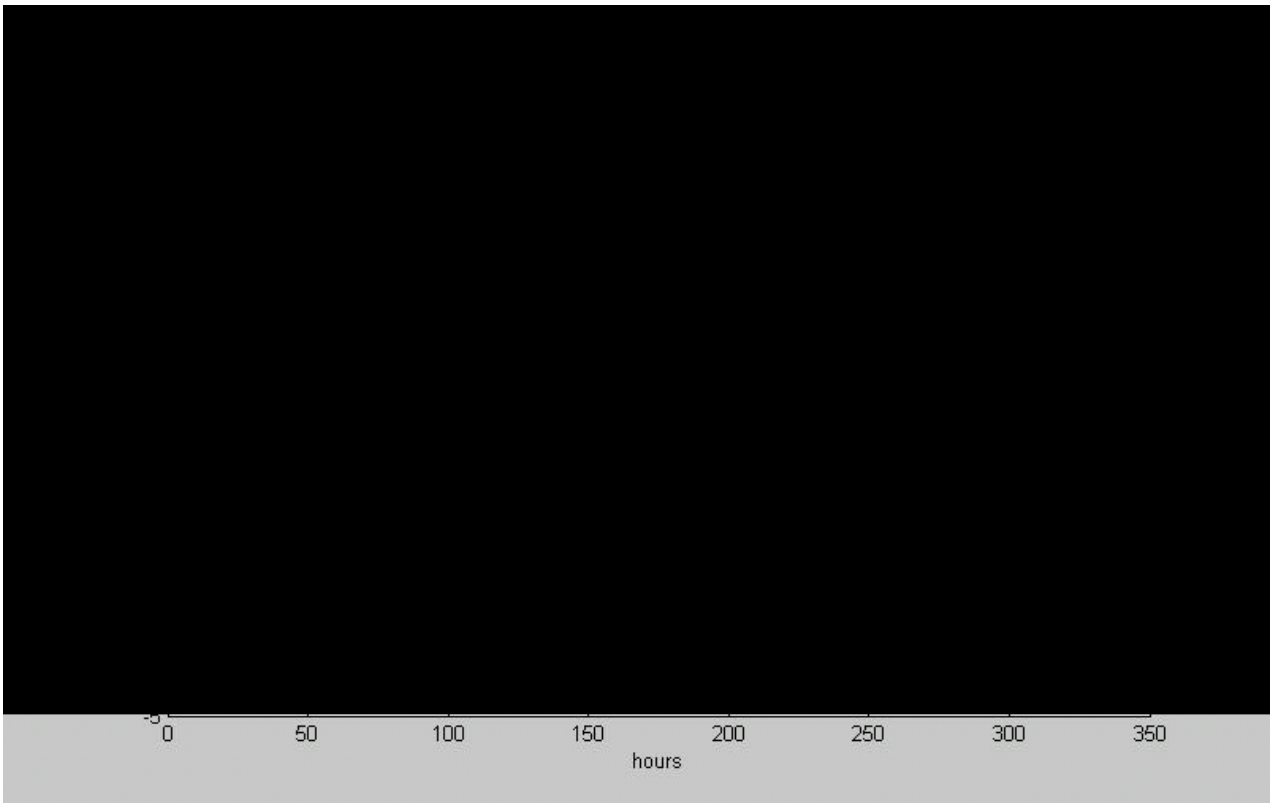
-5
0
50
100
150
200
250
300
350
hours


hours

7.3 First Flight Experiment

Shown in graphs 67-74 are the results of the flight experiment, carried out according to *Scenario A*. The TechSat MGM telemetry, accumulated over 35 revolutions, was processed by the Ground Estimator (GE), the relevant plots of the attitude state vector estimates being put in black. The estimates obtained by the onboard EKF, when available, are given in red.

As can be seen, at the beginning of the experiment, under the *COMPASS* control with Hw ≈ -0.05 Nt*m*s (see Graph 73), the satellite kept 3-axis stabilization, with φ, θ, and ψ amplitudes within 3°÷5°. Shortly after turning off the momentum wheel, at 18050th revolution, a dramatic increase of the satellite's angular velocity components occurred, mainly in its ω_x and ω_z components, unlike the simulation. In the *Torque-free rotation* phase, that lasted from 18052nd till the beginning of 18065th revolution, this pattern didn't change much. In the *No Wheel* phase, ω_z having the largest value, the satellite seems to rotate mainly about its nominally nadir-pointing axis.

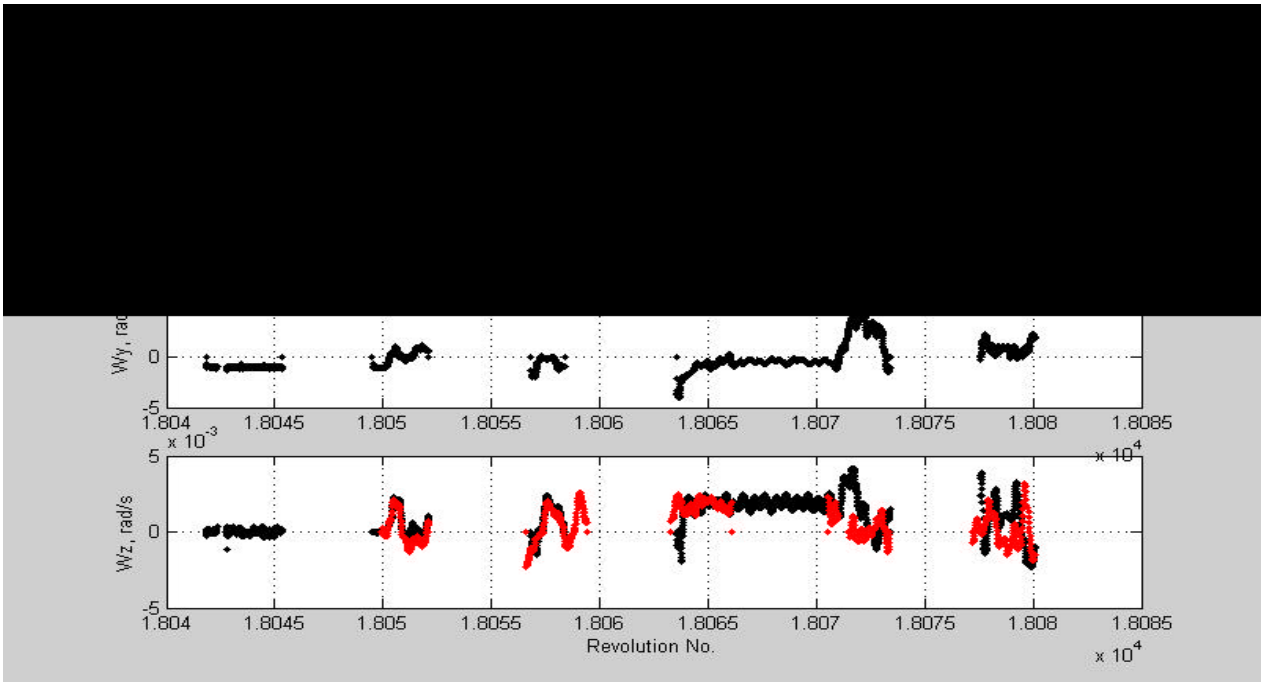

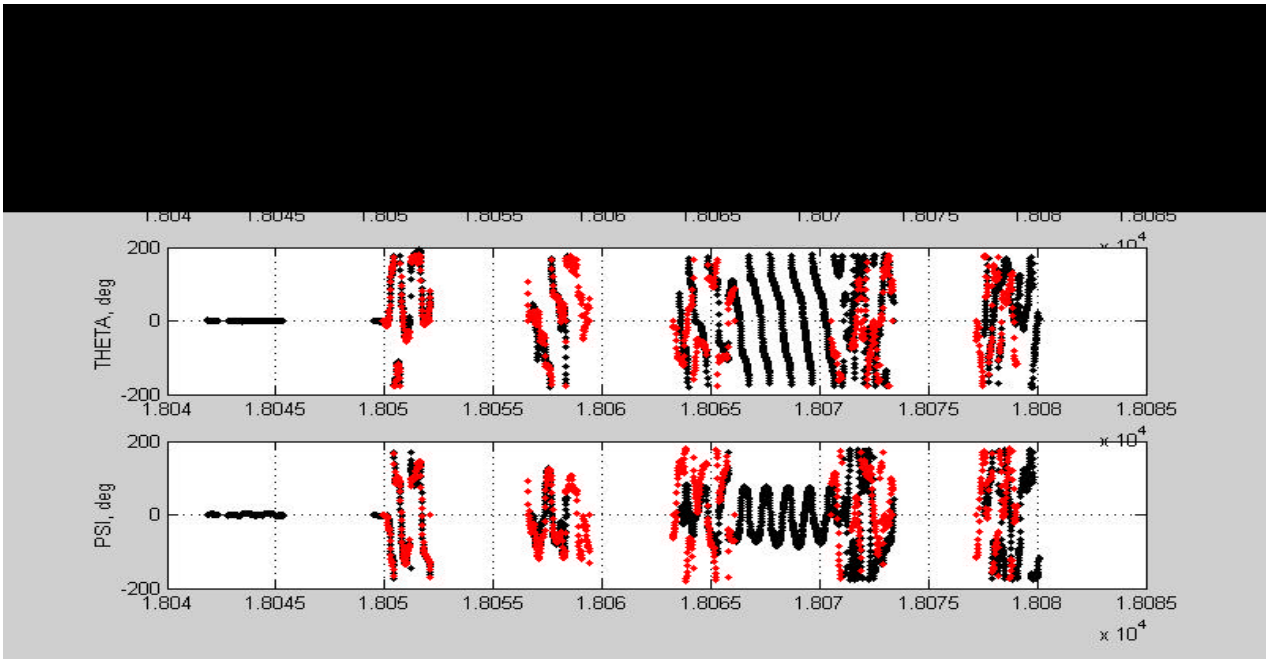

In graph 74, the estimates of the MGM biases, made by GE, are plotted: X-component - in red, Y- in green, and Z- in blue. The improbably large values of the MGM biases can be considered as an evidence of the inadequate EKF performance in the *Torque-free* and *No Wheel* phases.

Obviously, with the satellite's angular velocity that large, the estimates provided by EKF can't be considered as adequate. In addition, visible in the graphs are discrepancies between the estimates of the onboard EKF and GE, that can be attributed both to the gaps in the MGM telemetry available for GE, and to some differences in the two implementations of the EKF algorithm.

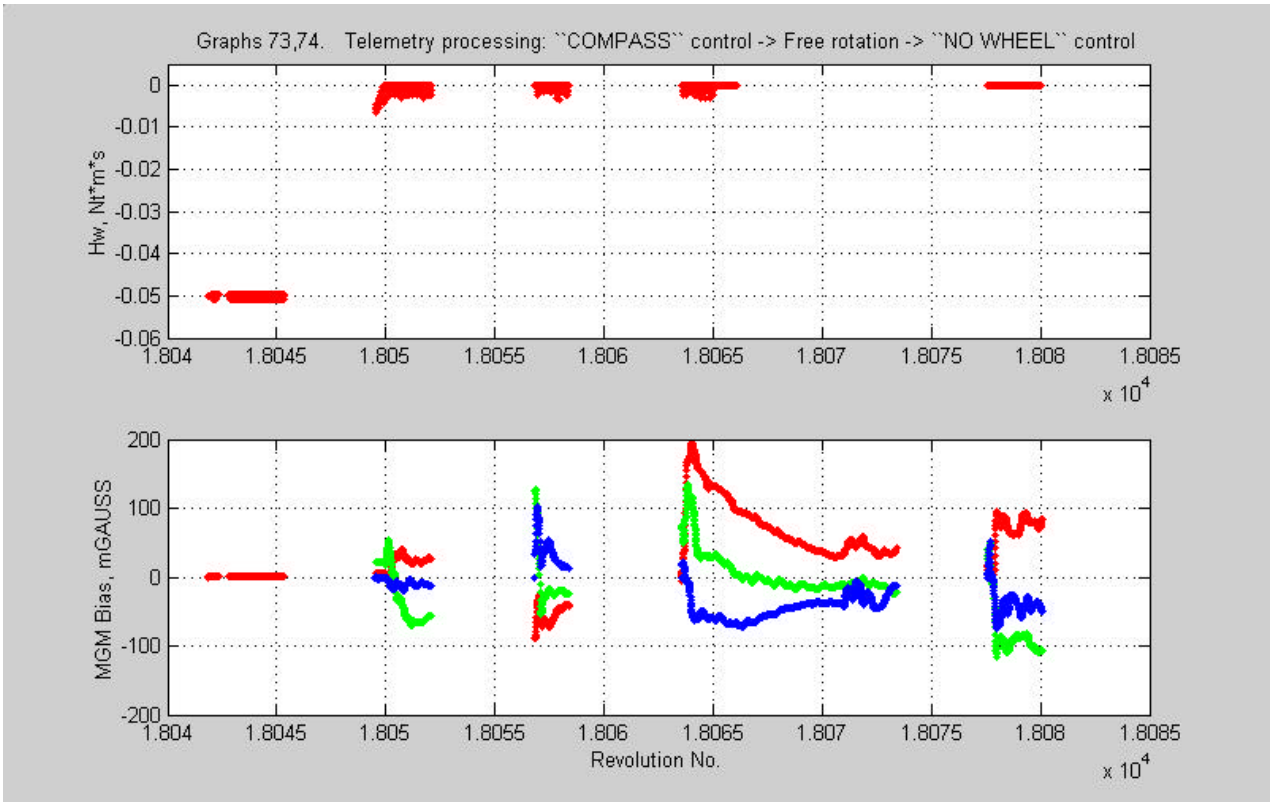

Actually, the state vector estimates only reflect the facts that could be stated immediately, comparing the expected and measured GMF vectors at the different phases of the experiment. The Graphs 75,76,77 display two sets of data, pertaining to *COMPASS* control and *Torque-free rotation* phases, and Graphs 78,79,80 – to the *No Wheel* phase. The expected vectors are plotted in black, while the measured ones – in red.

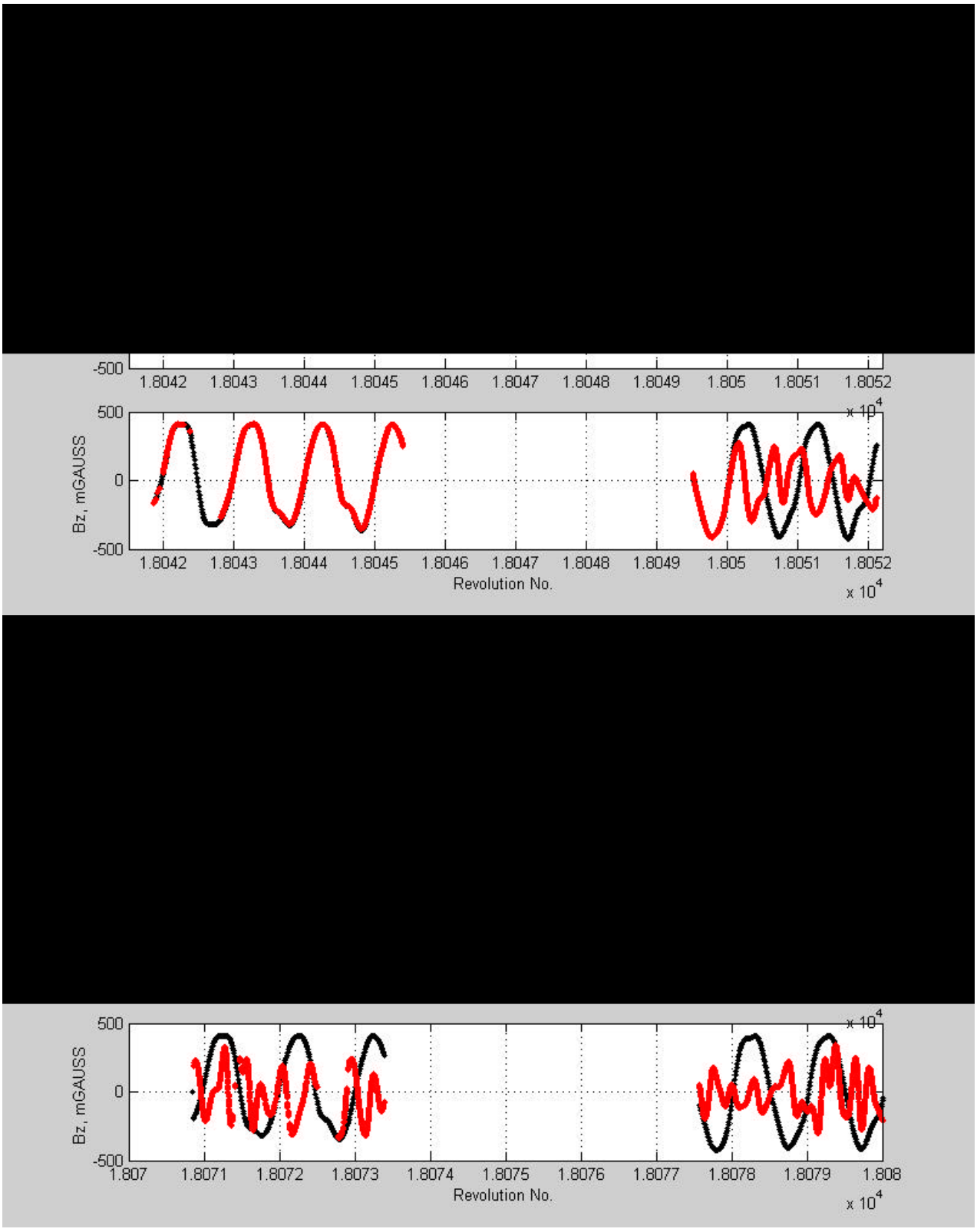
-500
1.8042
1.8043
1.8044
1.8045
1.8046
1.8047
1.8048
1.8049
1.805
1.8051
1.8052
x 10^4
500
0
-500
Bz, mGAUSS
Revolution No.
x 10^4
500
0
-500
Bz, mGAUSS
1.807
1.8071
1.8072
1.8073
1.8074
1.8075
1.8076
1.8077
1.8078
1.8079
1.808
Revolution No.
x 10^4

7.4 Second Flight Experiment

After fixing the problem with two EKF implementations, the new experiment was staged, to test the possibility of smooth transition from the weak (once per 10^s) *COMPASS* control to *Torque-free* rotation as specified in the *Scenario B*. Without this transition implemented, it makes no sense to switch to the *No wheel* control.

The results of this experiment are displayed in graphs 81-88, based on the telemetry that comprises about 40 TechSat revolutions. The switch of the *COMPASS* control to *Free rotation* took place at the revolution No.19021. Again, as in the previous experiment, soon after turning the MW off the tumbling began, as is confirmed by all the graphs. Now the discrepancies between the graphs pertaining to the onboard EKF and GE performance, are caused either by the gaps in the MGM telemetry downloaded for processing by GE, or by re-initialization of the onboard EKF, as in case of the mismatch seen near the revolutions 19020 and 19035.

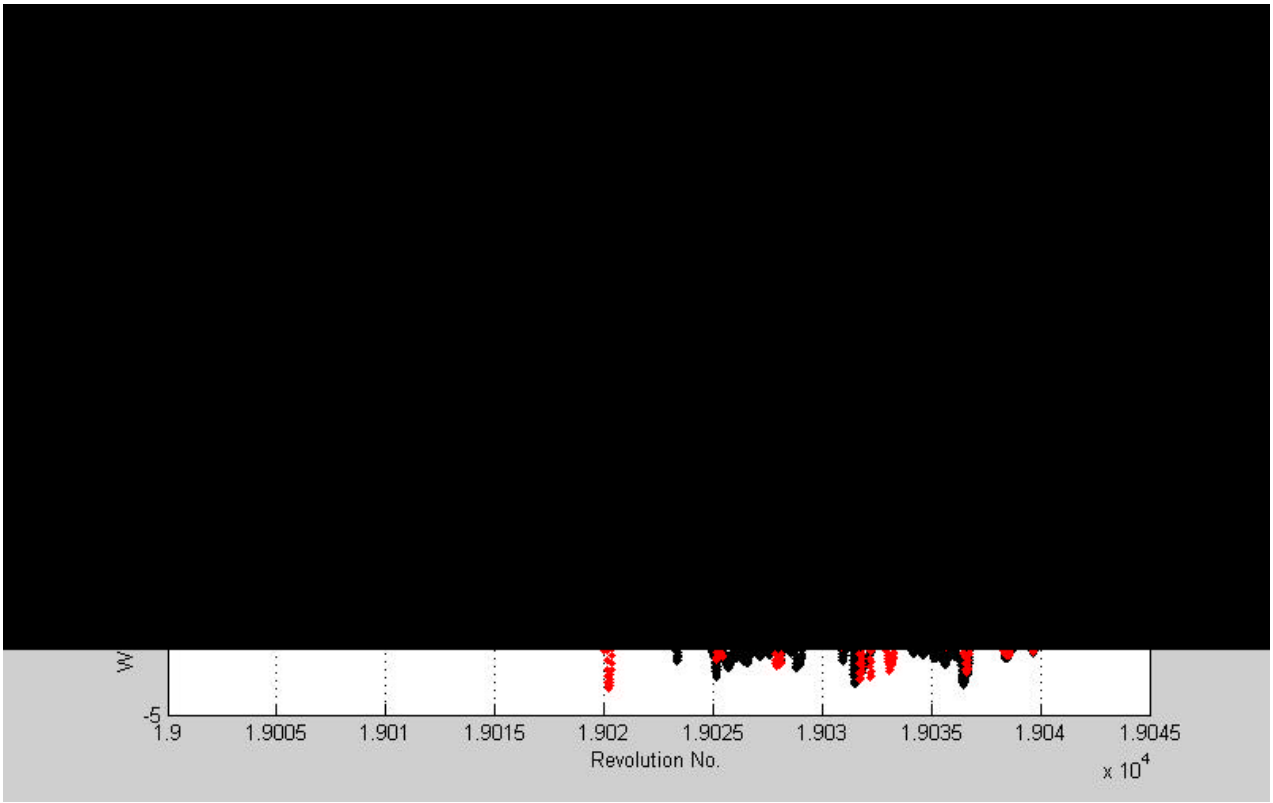

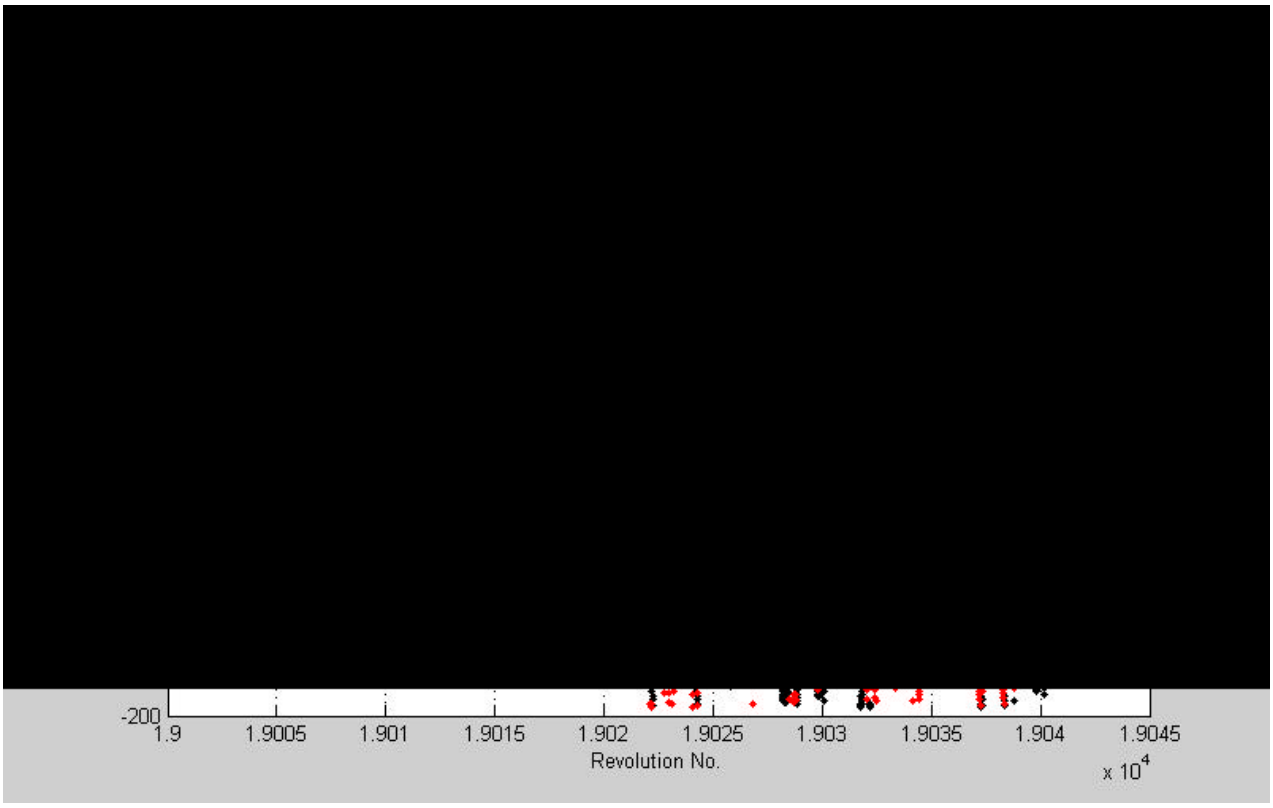
-200
1.9
1.9005
1.901
1.9015
1.902
1.9025
1.903
1.9035
1.904
1.9045
Revolution No.
x 10^4

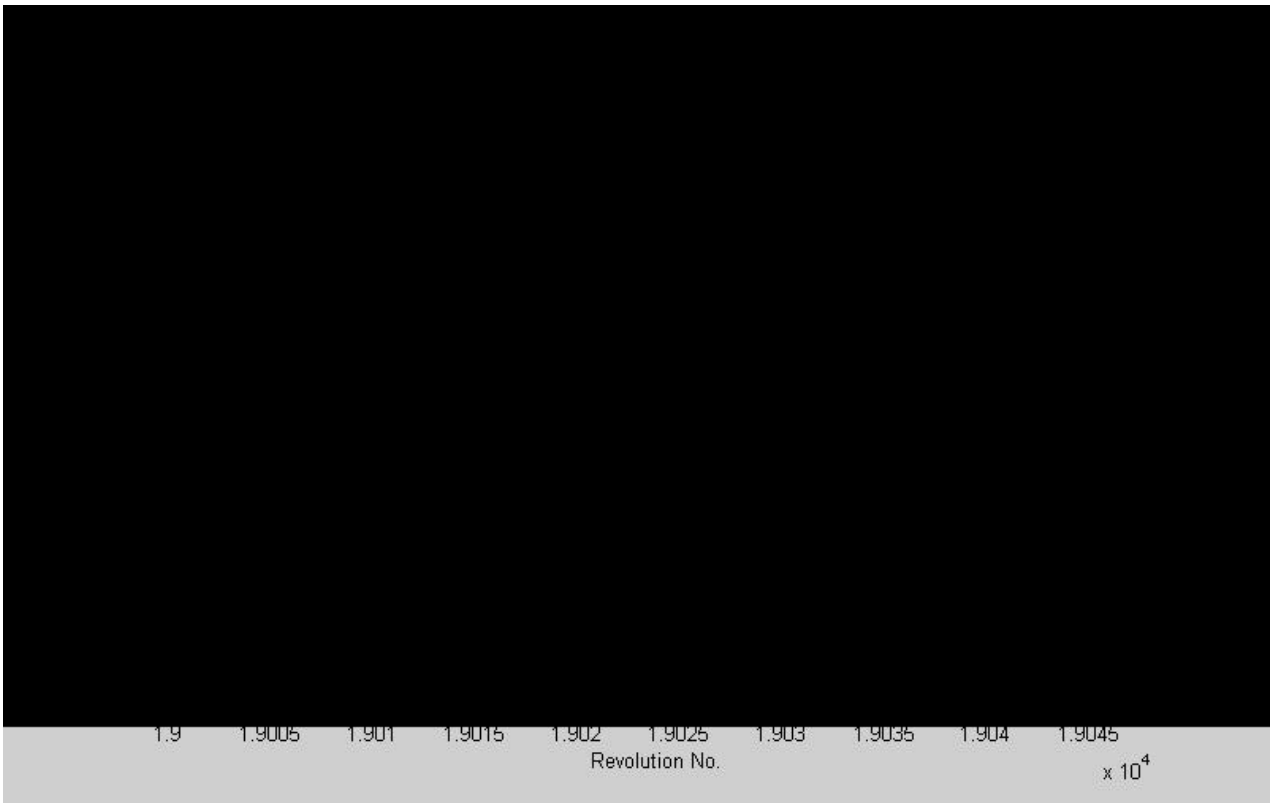
1.9
1.9005
1.901
1.9015
1.902
1.9025
1.903
1.9035
1.904
1.9045
Revolution No.
x 10^4

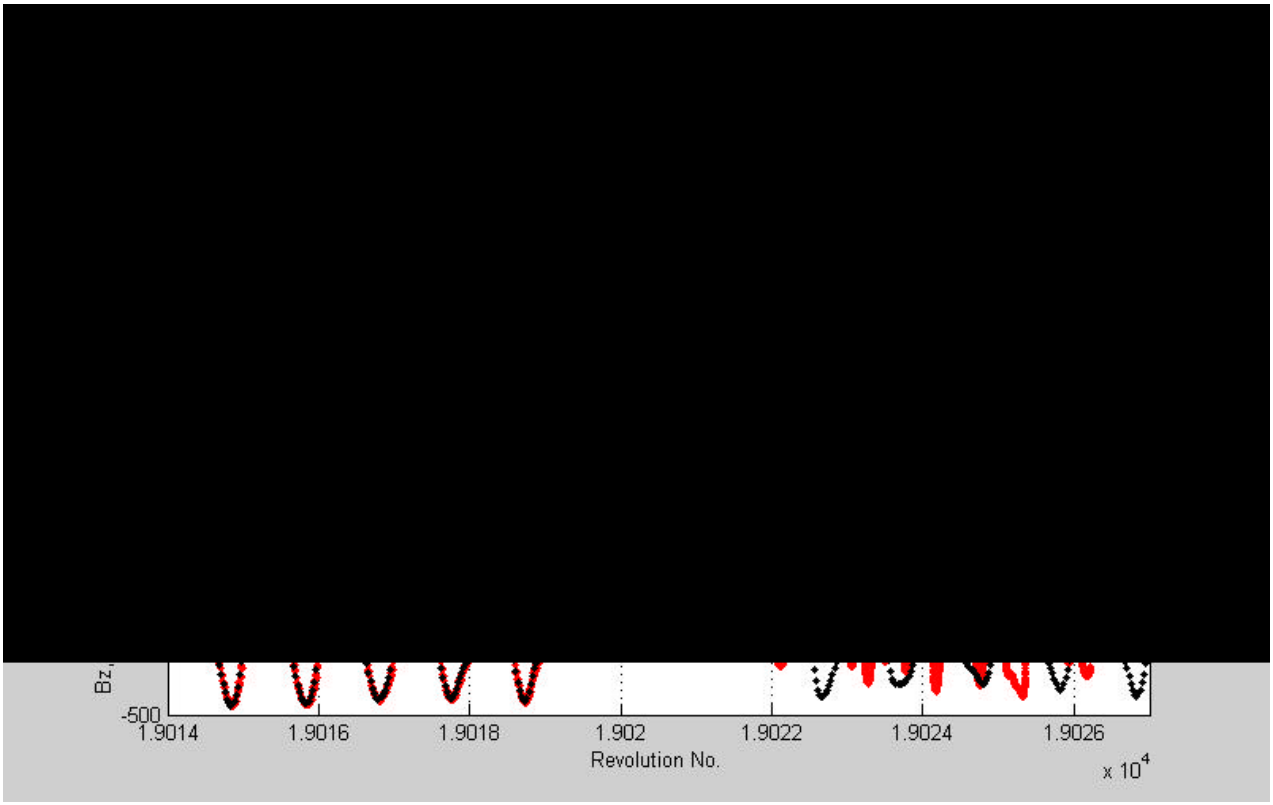

8. Summary and Conclusions

Work was performed with mixed results. On the one hand, the principal aims of the research were not achieved, in the sense that none of the attempts to stabilize TechSat in actual flight tests by any of the two PMC controllers available was successful. On the other hand, there are also some important accomplishments that can be of use both in further experiments with the TechSat, while alive, and in the possible testing of these or similar algorithms on other satellites. They are as follows:

1. As shown both in the simulations and in the flight tests, the proportional-plus-derivative *COMPASS* control law can provide a 3-axis stabilization of the satellite even with a very small momentum wheel's momentum bias of about –0.005 Nt.m.s;
2. The algorithmic sequences, involved in the Extended and Linear Kalman filters, were properly modified, to enable the filters' performance in the TechSat low-capacity onboard computer;
3. The attitude control scenarios were worked out and tested, that provide a smooth transition from the nominal control, with non-zero momentum bias, via wheel's slowing down and stopping, to a purely magnetic control.

It is quite probable, that both the algorithms would perform well, if they were actuated on the satellite without the momentum wheel, or with a wheel kept fixed after the satellite's release from the launcher. With regard to the case at hand, it is known, that neither the TechSat MW itself, nor the whole satellite's electric circuitry have ever been tested under conditions different from the nominal ones. This resulted in the inability to properly model two main sources of perturbations:

a. Sudden changes in the MW angular velocity near zero;
b. Additional magnetic dipole created by the MW coil that also can vary by some unpredictable way. Such a dipole, being collinear with BF Y-axis, would generate parasitic torques, affecting φ and ψ angles.

These perturbations affected both the MGM measurements and TechSat attitude during the experiments.

To conclude, one could say, that while TechSat is alive, and with the experience gained, it seems quite feasible to stage some new experiments that could unravel its, sometimes, enigmatic behavior.

9. References

1. Psiaki, M.L., "Magnetic Torquer Attitude Control Via Asymptotic Periodic Linear Quadratic Regulation," *Journal of Guidance, Control, and Dynamics*, Vol. 24, No. 2, 2001, pp. 386-394.
2. Mortensen R.E. ``A globally stable linear attitude regulator``, *Int. Journal of Control*, Vol. 8, No.3, 1968, pp. 297-302.
3. Karmanov, G., Shiryaev, A., "The TechSat-1 attitude estimation by telemetry processing", in Proceedings of the 39th Israel Annual Conference on Aerospace Sciences, Israel, Feb. 1999, pp.411-415.
4. Rozanov, M., Shiryaev, A., "Different Techniques for Gurwin-TechSat attitude assessment", in Proceedings of the 41th Israel Annual Conference on Aerospace Sciences, Israel, Feb. 2001. pp.504-508.
5. Friedland, B., "Control System Design: An Introduction to State-Space Methods", Mc-Graw-Hill Book Company, 1986.
6. Yunck, T.P., "Orbit Determination", in: "Global Positioning System: Theory and Applications"; Progress in Astronautics and Aeronautics, vol. 164, chapter 21, 1986.